PRIFYSGOL BANGOR / BANGOR UNIVERSITY

Thermophilic Carboxylesterases from Hydrothermal Vents of the Volcanic Island of Ischia Active on Synthetic and Biobased Polymers and Mycotoxins

Distaso, Marco; Chernikova, Tatyana; Bargiela, Rafael; Coscolín, Cristina; Stogios, Peter J.; Gonzalez-Alfonso, Jose L. ; Lemak, Sofia; Khusnutdinova, Anna; Plou, Francisco J.; Evdokimova, Elena; Savchenko, Alexei; Lunev, Evgenii; Yakimov, Michail M; Golyshina, Olga; Ferrer, Manuel; Yakunin, Alexander; Golyshin, Peter

Applied and Environmental Microbiology

DOI:
10.1128/aem.01704-22

Published: 28/02/2023

Peer reviewed version

Cyswllt i'r cyhoeddiad / Link to publication

Dyfyniad o'r fersiwn a gyhoeddwyd / Citation for published version (APA):
Distaso, M., Chernikova, T., Bargiela, R., Coscolín, C., Stogios, P. J., Gonzalez-Alfonso, J. L., Lemak, S., Khusnutdinova, A., Plou, F. J., Evdokimova, E., Savchenko, A., Lunev, E., Yakimov, M. M., Golyshina, O., Ferrer, M., Yakunin, A., & Golyshin, P. (2023). Thermophilic Carboxylesterases from Hydrothermal Vents of the Volcanic Island of Ischia Active on Synthetic and Biobased Polymers and Mycotoxins. *Applied and Environmental Microbiology*, *89*(2), e0170422. https://doi.org/10.1128/aem.01704-22

Hawliau Cyffredinol / General rights
Copyright and moral rights for the publications made accessible in the public portal are retained by the authors and/or other copyright owners and it is a condition of accessing publications that users recognise and abide by the legal requirements associated with these rights.

- Users may download and print one copy of any publication from the public portal for the purpose of private study or research.
- You may not further distribute the material or use it for any profit-making activity or commercial gain
- You may freely distribute the URL identifying the publication in the public portal ?

Take down policy
If you believe that this document breaches copyright please contact us providing details, and we will remove access to the work immediately and investigate your claim.

26. Apr. 2024

Thermophilic carboxylesterases from hydrothermal vents of the volcanic island of Ischia active on synthetic and biobased polymers and mycotoxins

Marco A. Distaso[a], Tatyana N. Chernikova[a], Rafael Bargiela[a], Cristina Coscolín[b], Peter Stogios[c], Jose L. Gonzalez-Alfonso[b], Sofia Lemak[c], Anna N. Khusnutdinova[a], Francisco J. Plou[b], Elena Evdokimova[c], Alexei Savchenko[c,d], Evgenii A. Lunev[a,e], Michail M. Yakimov[f], Olga V. Golyshina[a], Manuel Ferrer[b,‡], Alexander F. Yakunin[a,c,‡], and Peter N. Golyshin[a,*,‡]

[1]Centre for Environmental Biotechnology, School of Natural Sciences, Bangor University, Bangor, UK

[b]Department of Applied Biocatalysis, ICP, CSIC, Madrid, Spain

[c]Department of Chemical Engineering and Applied Chemistry, University of Toronto, Toronto, Canada

[d]Department of Microbiology Immunology and Infectious Diseases. University of Calgary, Calgary, Canada

[e]Institute of Gene Biology, Russian Academy of Sciences, Moscow, Russia

[f] Institute of Polar Sciences (ISP), CNR, Messina, Italy

‡Equal contributions.

*Corresponding authors at: the Centre for Environmental Biotechnology, Bangor University, LL57 2UW Bangor, UK (P.N. Golyshin); ICP, CSIC, Marie Curie 2, 28049 Madrid, Spain (M. Ferrer).

E-mail addresses: mferrer@icp.csic.es (M. Ferrer), p.golyshin@bangor.ac.uk (P.N. Golyshin)

Phone numbers: +34915854872 (M. Ferrer), +441248383629 (P.N. Golyshin)

KEYWORDS: Thermophilic bacteria, hydrothermal vents, Ischia, metagenome screening, carboxylesterase, polyesterase, 3PET, PLA, biochemical characterisation, crystal structure

ABSTRACT

Hydrothermal vents are geographically widespread and host microorganisms with robust enzymes useful in various industrial applications. We examined microbial communities and carboxylesterases of two terrestrial hydrothermal vents of the volcanic island of Ischia (Italy) predominantly composed of Firmicutes, *Proteobacteria* and *Bacteroidota*. High-temperature enrichment cultures with the polyester plastics polyhydroxybutyrate (PHB) and polylactic acid (PLA) resulted in an increase of *Thermus* and *Geobacillus* spp., and to some extent, *Fontimonas* and *Schleiferia* spp. The screening at 37-70ºC of metagenomic fosmid libraries from above enrichment cultures identified three hydrolases (IS10, IS11 and IS12), all derived from yet uncultured Chloroflexota and showing low sequence identity (33-56%) to characterized enzymes. Enzymes expressed in *Escherichia coli* exhibited maximal esterase activity at 70-90ºC, with IS11 showing the highest thermostability (90% activity after 20 min incubation at 80ºC). IS10 and IS12 were highly substrate-promiscuous and hydrolysed all 51 monoester substrates tested. Enzymes were active with PLA, polyethylene terephthalate model substrate, 3PET, and mycotoxin T-2 (IS12). IS10 and IS12 had a classical α/β hydrolase core domain with a serine hydrolase catalytic triad (Ser155, His280, Asp250) in their hydrophobic active sites. The crystal structure of IS11 resolved at 2.92 Å revealed the presence of the N-terminal β-lactamase-like domain and C-terminal lipocalin domain. The catalytic cleft of IS11 included catalytic Ser68, Lys71, Tyr160, and Asn162, whereas the lipocalin domain enclosed the catalytic cleft like a lid contributing to substrate binding. Our study has identified novel thermotolerant carboxylesterases with a broad substrate range, including polyesters and mycotoxins, for potential applications in biotechnology.

IMPORTANCE

High-temperature-active microbial enzymes are important biocatalysts for many industrial applications including recycling of synthetic and biobased polyesters increasingly used in textiles, fibres, coatings and adhesives. Here, we have discovered three novel thermotolerant carboxylesterases (IS10, IS11 and IS12) from high-temperature enrichment cultures from Ischia hydrothermal vents incubated with biobased polymers. The identified metagenomic enzymes originated from uncultured Chloroflexota and showed low sequence similarity to known carboxylesterases. Active sites of IS10 and IS12 had the largest "effective volumes" among the characterized prokaryotic carboxylesterases and exhibited high substrate promiscuity, including hydrolysis of polyesters and mycotoxin T-2 (IS12). Though less promiscuous compared to IS10 and IS12, IS11 had a higher thermostability with high temperature optimum (80-90 ºC) for activity, hydrolysed polyesters, and its crystal structure revealed an unusual lipocalin domain likely involved in substrate binding. The polyesterase activity of these enzymes makes them attractive candidates for further optimisation and potential application in plastics recycling.

INTRODUCTION

Environmental microbial communities and microorganisms represent an enormous reserve of biochemical diversity and enzymes for fundamental research and applications in biotechnology (1,2). However, the vast majority of environmental microbes have never been grown and characterised in the laboratory (3,4). The metagenomic approach has emerged as a strategic way to study unculturable microorganisms and their enzymes using various computational and experimental methods (5-7). Metagenomics includes shotgun sequencing of microbial DNA purified from a selected environment, high-throughput screening of metagenomic expression libraries (functional metagenomics), profiling of RNAs and proteins produced by a microbial community (meta-transcriptomics and meta-proteomics), and identification of metabolites and metabolic networks of a microbial community (meta-metabolomics) (8). Global DNA sequencing efforts and several large-scale metagenome sampling projects revealed the vast sequence diversity in environmental metagenomes and microbial genomes, as well as the presence of numerous unknown or poorly characterised genes (9-12). For example, a high-throughput project focused on carbohydrate-active enzymes has identified over 27,000 related genes and demonstrated the presence of glycoside hydrolase activity in 51 out of 90 tested proteins (13). Other large scale metagenomic projects include the Sargasso Sea sampling (over one million new genes discovered), the Global Ocean Survey (over six million genes), and human gut microbiome (over three million genes) (9-12). Thus, through the advent of metagenomics, we are starting to generate insights into the rich microbial worlds thriving in different environments. Nevertheless, a recent analysis of metagenome screening studies suggested that all representative types of environmental habitats (terrestrial, marine, and freshwater) are under-sampled and under-investigated (14). It is estimated that total number of microbial cells is 10^{30}, whereas the natural protein universe exceeds 10^{12} proteins indicating that our knowledge of proteins and biochemical diversity on Earth is very limited (15-17). Therefore, the determination of protein function or enzyme activity for millions of genes of unknown function and biochemically uncharacterised proteins represents one of the main challenges of the postgenomic biology.

The approaches of experimental metagenomics include meta-transcriptomics, meta-proteomics, metabolomics, and enzyme screening (6,7,17-19). Activity-based screening of metagenome gene libraries represents a direct way for tapping into the metagenomic resource of novel enzymes. This approach involves expressing genes from metagenomic DNA fragments in heterologous hosts, commonly *Escherichia coli*, and assaying libraries of clones on agar plates for enzymatic activities using chromogenic or insoluble substrates (18). Importantly, this approach offers the possibility to identify novel families of enzymes with no sequence similarity to known enzymes. Screening of metagenome gene libraries from different terrestrial, marine, and freshwater environments has already expanded the number of new enzymes including novel nitrilases, glycoside hydrolases, carboxyl esterases, and laccases (14,20,21).

Carboxylesterases (EC 3.1.1.1) are a diverse group of hydrolytic enzymes catalysing the cleavage and formation of ester bonds, which represent the third largest group of industrial biocatalysts (after amylases and proteases). Many esterases show a wide substrate range and high regio- and stereo-selectivity making them attractive biocatalysts for applications in pharmaceutical, cosmetic, detergent, food, textile, paper and biodiesel industries (22,23).

Most of known carboxylesterases belong to the large protein superfamilies of α/β hydrolases and β-lactamases and have been classified into 46 subfamilies (including 11 true lipase subfamilies)based on sequence analysis (22,24,25). A significant number of these enzymes have been characterised both biochemically and structurally, because they are of high interest for biotechnological applications (22,23,26). Screening of metagenome gene libraries and genome mining has greatly expanded the number of novel carboxylesterases including enzymes active against aryl esters or polymeric esters (polyesterases) (21-23,26,27). However, the increasing demand for environmentally friendly industrial processes has stimulated research on the discovery of new enzymes and their application as biocatalysts to meet the challenges of a circular bioeconomy (28,29). The global enzyme market is expected to grow from $8.18 billion in 2015 to $17.50 billion by 2024 (28). However, the majority of known enzymes are originated from mesophilic organisms, which have limited stability under harsh industrial conditions including high temperatures, extreme pH, solvents, and salts (30,31). Thus, the discovery of robust enzymes including carboxylesterases and engineering of more active variants represent the key challenges for the development of future biocatalytic processes. Extremophilic microorganisms are an attractive source of industrial biocatalysts, because they evolved robust enzymes that function under extreme conditions (high/low temperatures, high/low pH, salts) (14,26,30,32). In addition, extremophilic enzymes found in one environment are typically also tolerant to other extreme conditions making them attractive biocatalysts for various applications including depolymerization of synthetic polymers and inactivation of mycotoxins (32-36).

Hydrothermal vents are extreme environments located in tectonically active sites, which are classified as terrestrial and marine (deep-sea and shallow-sea) systems (37). Hydrothermal vents are characterised by harsh physico-chemical conditions (high temperature and low pH) and are known as source of thermophilic microbes and enzymes with biotechnological importance. Although terrestrial hydrothermal vents have relatively easy access, they remain under-investigated compared to (sub)marine hydrothermal vents. To provide insights into microbial diversity of terrestrial hydrothermal vents, we analysed the natural microbial communities of two thermophilic hydrothermal vents located on the volcanic island of Ischia (Italy), as well as the effect of polyester plastic addition on these microbial communities using barcoded DNA sequencing of extracted DNA. Using activity-based metagenomic approach, we screened fosmid libraries for carboxylesterase activity using tributyrin agar plates, identified 14 unique fosmids encoding putative hydrolases, from which three soluble carboxylesterases (IS10, IS11, and IS12) were recombinantly produced in *E. coli* and biochemically characterised including substrate range and stability using both monoester and polyester substrates. The crystal structure of IS11 was resolved to reveal the N-terminal β-lactamase-like serine hydrolase domain connected to the C-terminal lipocalin domain. The active site of IS11 accommodated the conserved catalytic residues Ser68, Lys71, Tyr160, and Asn162, as well as numerous hydrophobic residues potentially involved in substrate binding. Structural models of IS10 and IS12 revealed classical α/β hydrolase domains with a catalytic serine hydrolase triad (Ser155, His280, Asp250), multiple hydrophobic residues in their active sites with the largest “effective volumes” reported for prokaryotic carboxylesterases.

MATERIALS AND METHODS

Environmental sampling sites and enrichment cultures. Sediment samples with water were collected in September 2018 from the geothermal areas of the volcanic island of Ischia (the Gulf of Naples, Italy). The samples were taken from the Cavascura hydrothermal springs (40.70403 13.90502): IS1 (pH 8.5, 45 ºC) and IS2 (pH 7.0, 55 ºC); and from the sandy fumaroles of Maronti beach near St Angelo (40.70101 13.89837): IS3 (pH 4.5, 75 ºC) and IS4 (pH 5.0, 75 ºC). For each sample, triplicate enrichment cultures were established containing different polymers or plastics as substrates, polylactic acid film (PLA, poly-D,L-lactide, M_w 10,000-18,000 Da), polyhydroxybutyrate (PHB) and a commercial compostable polyester blend (P3, Blend), kindly provided by the Biocomposites Centre, Bangor University, UK. Plastic films cut (3 mm x 20 mm), washed in 70 % ethanol and air-dried were added to samples. For IS1 and IS2 cultures, modified DSMZ medium 1374 (https://bacmedia.dsmz.de/medium/1374) was used, which contained (g L^{-1}): NaCl, 1; $MgCl_2 \cdot 6H_2O$, 0.4; KCl, 0.1; NH_4Cl, 0.25; KH_2PO_4, 0.2; Na_2SO_4, 4; $NaHCO_3$, 0.1; $CaCl_2 \cdot 2H_2O$, 0.5. The medium was adjusted to pH 7.5 with 10N NaOH. For IS3 and IS4 cultures, modified DSMZ medium 88 (https://bacmedia.dsmz.de/medium/88) was used, which contained (g L^{-1}): $(NH_4)_2SO_4$, 1.3; KH_2PO_4, 0.28; $MgSO_4 \cdot 7H_2O$, 0.25; $CaCl_2 \cdot 2H_2O$, 0.07. The medium was adjusted to pH 4.5 with 10N H_2SO_4. Additionally, the trace element solution SL-10 (from DSMZ medium 320 https://bacmedia.dsmz.de/medium/320) was added at 1:1000 (vol/vol) to both media. Enrichment cultures contained 0.5 g of sample sediment and 0.25 g of a polymer in 10 mL of growth medium. The cultures were incubated at 50 °C (IS1-IS2) or 75 °C (IS3-IS4) with slow agitation (30 rpm) for 4 days, then culture aliquots (20% of the volume of enrichment cultures) were transferred to a fresh medium and incubated for 11 days under the same conditions (Table S1).

DNA extraction and 16S rRNA amplicon sequencing. Prior to DNA extraction, the enrichment cultures (9 mL each) were vortexed and biomass was collected by centrifugation at 10,000 rcf for 10 min at 4 °C. The pellets were resuspended in 250 µL of sterile phosphate-buffered saline (PBS, pH 7.5) and transferred to 1.5 mL tubes. High molecular weight DNA was obtained using the ZymoBIOMICS DNA Miniprep Kit (Zymo Research, Irvine, Ca, USA) in accordance with manufacturer's instructions. Finally, DNA was eluted with 50 µL of nuclease free water. The quality of extracted DNA was assessed by gel electrophoresis, and DNA concentration was estimated using Qubit™ 4.0 Fluorometer dsDNA BR Assay Kit (Life Technologies, USA). The Illumina-compatible libraries of hypervariable V4 region of 16S rRNA gene were prepared by single PCR with dual-indexing primer system with heterogeneity spacer as described previously (38). Modified forward primer F515 (5'-GTGBCAGCMGCCGCGGTAA-3') and reverse R806 prokaryotic primer (5'-GGACTACHVGGGTWTCTAAT-3') were used. PCR reactions were performed using MyTaq™ Red DNA Polymerase (Bioline) in a Bio-Rad® thermocycler with the following program: 95 °C for 2 min for denaturation followed by 30 cycles at 95 °C for 45 s, 50 °C for 60 s, 72 °C for 30 s, with a final elongation at 72 °C for 3 min. PCR products of approximately 440 bp were visualised by gel electrophoresis and gel-purified using the

QIAEX II Gel Extraction Kit® (QIAGEN). The purified barcoded amplicons were quantified by Qubit™ dsDNA BR Assay Kit (Life Technologies, USA), pooled in equimolar amounts and sequenced on Illumina MiSeq™ platform (Illumina Inc., San Diego, CA, USA) using paired-end 250 bp reads at the Centre for Environmental Biotechnology (Bangor, UK). Sequencing reads were processed and analysed as previously described (39). All statistical analysis was conducted using R programming environment (40) *prcomp* function and in-house scripts for graphical design.

Preparation of the Ischia metagenome library from polyester enrichment cultures. High molecular weight DNA extracted from all enrichment cultures was combined in equimolar amounts and used to prepare two metagenomic fosmid libraries 'IS_Lib1' (Cavascura enrichments) and 'IS_Lib2' (Maronti enrichments) using the CopyControl™ Fosmid Library pCC2FOS Production Kit (Epicentre Technologies, Madison, USA). DNA was end-repaired to generate blunt-ended 5'-phosphorylated fragments according to manufacturer's instructions. Subsequently, DNA fragments in the range of 30-40 kbp were resolved by gel electrophoresis (2 V cm^{-1} overnight at 4 °C) and recovered from 1% low melting point agarose gel using GELase 50X buffer and GELase enzyme (Epicentre). Nucleic acid fragments were then ligated to the linearized CopyControl pCC2FOS vector following the manufacturer's instructions. After the in vitro packaging into the phage lambda (MaxPlax™ Lambda Packaging Extract, Epicentre), the transfected phage T1-resistant EPI300™-$T1^R$ *E. coli* cells were spread on Luria-Bertani (LB) agar medium containing 12.5 µg mL^{-1} chloramphenicol and incubated at 37 °C overnight to determine the titre of the phage particles. The resulting library had estimated titre of $14x10^4$ and $1x10^4$ non-redundant fosmid clones in IS_Lib1 and IS_Lib2 libraries, correspondingly. For long-term storage, *E. coli* colonies were washed off from the agar surface using liquid LB medium containing 20 % (v/v) sterile glycerol and the aliquots were stored at −80 °C.

Activity-based screening of the polyester enrichment metagenome library for esterase activity. The metagenomic libraries were screened for carboxylesterase/lipase activity as follows. The fosmid library was grown on LB agar plates containing 12.5 µg mL^{-1} chloramphenicol at 37 °C overnight to yield single colonies. Then, 3,456 clones were arrayed in 9 x 384-well microtitre plates and cultivated at 37 °C in LB medium supplemented with 12.5 µg mL^{-1} chloramphenicol. Those original microtitre plates were stored at -80 °C after the addition of glycerol, at final concentration of 20 % (vol/vol). For screening clone libraries, 384-pin replicators were used to print clones onto the surface of large LB agar square plates (245 mm x 245 mm) containing 12.5 µg mL^{-1} chloramphenicol, 2 mL L^{-1} fosmid autoinduction solution (Epicentre), each plate contained 0.3 % (v/v) tributyrin (Sigma-Aldrich, Gillingham, UK) as described earlier (27). After an initial overnight growth at 37 °C, the LB agar plates were incubated for 48 hours at 37, 50 or 70 °C. Positive hits were confirmed by re-testing of the corresponding fosmid clones taken from the original microtitre plate.

Sequencing and analysis of metagenomic fragments. Positive fosmid clones were cultivated in 100 mL LB medium containing 12.5 µg mL^{-1} chloramphenicol and 2 mL L^{-1}

244 fosmid autoinduction solution (Epicentre) at 37 °C overnight. Biomass was collected by
245 centrifuging at 3,200 g for 30 min and fosmid DNA was extracted from the pellet using the
246 QIAGEN Plasmid Midi Kit (QIAGEN) following the manufacturer's instructions.
247 Approximate size of the cloned fragments was assessed on agarose gel electrophoresis after
248 double endonuclease digestion with *Xba*I and *Xho*I (New England Biolabs, Ipswich, MA,
249 USA). The Sanger sequencing of the termini of inserted metagenomic fragments of each
250 purified fosmid was done at Macrogen Ltd. (Amsterdam, The Netherlands) using standard
251 pCC2FOS sequencing primers (Epicentre). Non-redundant fosmids were selected, their DNA
252 concentrations were quantified by Qubit™ 4.0 Fluorometer dsDNA BR Assay Kit
253 (Invitrogen), pooled in equimolar amounts and prepared for Illumina MiSeq® sequencing.
254 Pooled DNA was fragmented using the Bioruptor Pico Sonicator (Diagenode, Denville, NJ,
255 USA) with parameters adjusted to obtain 400-600 bp fragments. The fragment library was
256 prepared using the NebNext Ultra II DNA Library preparation kit (New England Biolabs,
257 Ipswich, MA, USA) according to the manufacturer's instructions. The obtained library was
258 sequenced on MiSeq® platform (Illumina, San Diego, USA) using a microflow cell 300-
259 cycles V2 sequencing kit. Obtained paired end reads were subjected to quality filtering,
260 trimming and assembly as previously described (41). Gene prediction and primary functional
261 annotation were performed using the MetaGeneMark annotation software
262 (http://opal.biology.gatech.edu) (42). Translated protein sequences were annotated using
263 BLAST searches of UniProt and the non-redundant GenBank databases (43). Multiple
264 sequence alignments were generated using MUSCLE application (44) and visualised on
265 Geneious v.9 (Biomatters, New Zealand). The Neighbour-Joining and maximum likelihood
266 trees were constructed in MEGA X (45) using the settings for the Poisson model and
267 homogenous patterning between lineages. The bootstrapping was performed with 1,000
268 pseudoreplicates.

269 **Gene cloning, expression and purification of selected proteins.** Selected gene candidates
270 were amplified by PCR in a T100 Thermal Cycler (Bio-Rad) using Herculase II Fusion
271 Enzyme (Agilent, Cheadle, UK) with oligonucleotide primer pairs incorporating pET-46
272 Ek/LIC vector adapters (Merck, Darmstadt, Germany). PCR products were then purified and
273 cloned into the above pET-46 Ek/LIC vector harbouring an N-terminal 6xHis tag, as
274 described by the manufacturer. The DNA inserts in the resulting plasmids were verified by
275 Sanger sequencing at Macrogen Ltd. (Amsterdam, The Netherlands) and then transformed
276 into *E. coli* BL21(DE3) for recombinant protein expression. *E. coli* BL21(DE3) harbouring
277 pET-46 Ek/LIC plasmid were grown on LB medium to mid-log growth phase (OD_{600} 0.7-
278 0.8), induced with isopropyl-β-d-thiogalactopyranoside (IPTG, 0.5 mM) and incubated at 20
279 °C overnight. Cells were disrupted by sonication as reported earlier (46) and recombinant
280 proteins were purified using metal-chelate affinity chromatography on Ni-NTA His-bind
281 columns. Protein size and purity were assessed using denaturing gel electrophoresis (SDS-
282 PAGE), and protein concentration was measured by Bradford assay (Merck, Gillingham,
283 UK).

284 **Enzyme assays.** Carboxyl esterase activity of purified proteins against *p*-nitrophenyl (*p*NP)
285 or α-naphthyl (αN) esters was determined by measuring the amount of α-naphthol released
286 by esterase-catalysed hydrolysis essentially as described previously (27,46). Under standard

assay conditions the reaction mixture contained 50 mM potassium phosphate buffer (pH 7.0), 1 mM *p*NP-butyrate as substrate, and 0.2-1.8 µg of enzyme in a final volume of 200 µL. Reactions were incubated at 30 °C for 3-5 min and monitored at 410 nm (for *p*NP esters) or 310 nm (for αN esters). Non enzymatic hydrolysis of ester substrates was subtracted using a blank reaction with denatured enzyme. The effect of pH on esterase activity was evaluated using the following buffers: sodium citrate (pH 4.0 and 5.0), potassium phosphate (pH 6.0 and 7.0), Tris-HCl (pH 8.0 and 9.0). The activity was monitored at 348 nm (the pH-independent isosbestic wavelength of α-naphthol). The effect of temperature on esterase activity was studied using a range of temperatures (from 20 °C to 90 °C). In order to assess the thermal stability of purified esterases, the enzymes were dissolved in potassium phosphate buffer (pH 7.0) and preincubated at the indicated temperatures (from 30 to 95 ºC) for 20 min. The enzyme solutions were then cooled down on ice and the residual activity was measured under standard conditions (at 30 ºC). Substrate specificity of purified enzymes was analysed using model *p*NP- and αN-esters with different chain lengths: *p*NP-acetate (C2), αN-propionate (C3), *p*NP-butyrate (C4), αN-butyrate (C4), *p*NP-hexanoate (C6), *p*NP-dodecanoate (C12), and *p*NP-palmitate (C16), obtained from Sigma-Aldrich and Tokyo Chemical Industry TCI. Kinetic parameters for these substrates were determined over a range of substrate concentrations (0.012-4 mM; 30 ºC) and calculated by non-linear regression analysis of raw data fit to Michaelis-Menten function using GraphPad Prism software v.6. Hydrolysis of 44 soluble non-chromogenic monoester substrates (Table S2) and T-2 mycotoxin (Merck Life Science S.L.U., Madrid, Spain) was assayed at 37 ºC using a pH indicator assay with Phenol Red and monitored at 550 nm (47). The reaction products of enzymatic degradation of T-2 mycotoxin were analysed using reversed phase chromatography on a Waters 600 HPLC system, coupled to an autosampler (Waters, model 717plus), and equipped with a Zorbax Eclipse Plus C18 column (Agilent, 4.6 x 100 mm, 3.5 µm, 40 ºC) and an Evaporative Light Scattering Detector (ELSD, Sedere Sedex model 55). The reaction products were separated using gradient elution (1.0 ml/min) with acetonitrile and water (5%: 1 min, 5%-95%: 9 min, 95 %: 3 min, 5 %: 7 min). Polyester depolymerization activity of purified proteins against 3PET (bis(benzoyloxyethyl) terephthalate) was measured using 1.5 % agarose plates containing 0.2 % of emulsified polyesters. 3PET was purchased from CanSyn Chem. Corp. (Toronto, Canada). Agarose plates with emulsified 3PET were prepared as described previously (48). After protein loading, the plates were sealed and incubated at 37 ºC for 1-5 days. The presence of polyesterase activity was indicated by the formation of a clear zone around the wells with proteins. Apart from plate assays, activity assays of IS10, IS11 and IS12 for 3PET suspension hydrolysis were performed in 50 mM Tris-HCl buffer, pH 8.0, at 30 °C, in a shaker at 600 rpm, the final reaction volume for each experiment was 0.2 mL, and the final protein amount 50 µg. The reactions were terminated after 13 h by filtering reaction mixture on a 10 kDa spin filter. 10 µL of filtrate was analysed using the high-performance liquid chromatography system (HPLC), Schimadzu, Prominence-I (Milton Keynes, UK) equipped with a Schimadzu C18 Shim-pack column (4.6 × 150 mm, 5 µm). The mobile phase was 25 % (vol/vol) methanol with 0.1 % (vol/vol) H_3PO_4 in HPLC-grade water at a flow rate of 0.7 mL min^{-1} for 2 min, following increase to 55 % of methanol to 118 min, followed by 25 % methanol at 22 min; the effluent was monitored at the wavelength of 240 nm, the column was conditioned at

331 40 ºC. The hydrolytic products of mono(2-hydroxyethyl)terephthalic acid (MHET), bis(2-
332 hydroxyethyl)terephthalate (BHET) and terephthalic acid (TPA) were identified by
333 comparing the retention times with their standards, and reactions without enzyme were
334 served as negative controls. All samples of each experiment were analysed in triplicate.

335 **Enzymatic activity against PLA.** Hydrolysis of PLA was assayed by measurement of lactic
336 acid production as follows: 5 mg of each PLA (all, acid-terminated and purchased from
337 PolySciTech (W. Lafayette, USA)), P(D)LA 10-15,000 Da, P(D,L,)LA (Resomer R202H, 10-
338 18,000 Da) or P(L)LA 15-25,000 Da) suspended in 0.5 mL of 0.4 M Tris-HCl (pH 8.0) were
339 mixed with 50 µg of purified enzyme and incubated for 48 h at 37 ºC with shaking (1000
340 rpm). Samples were then centrifuged at 12,000 g for 5 min at 4 ºC. 200 µl of supernatant
341 were mixed with 200 µl of mobile phase (0.005 N H_2SO_4). Sample was filtered through 13
342 mm Millipore PES syringe membrane filter (0.02 µm pore diameter) and analysed by HPLC
343 Shimadzu, Prominence-I (Milton Keynes, UK) with an ion exchange column Hi PlexH (300
344 x 7.7 mm) (Agilent, Cheadle, UK) and 0.6 mL min^{-1} flow rate at 55 ºC (oven temperature)
345 with UV detector set at 190-210 nm.

346 **Protein crystallization and structure determination.** Native metagenomic esterases were
347 purified using metal-chelate affinity chromatography, and crystallization was performed at
348 room temperature using the sitting-drop vapor diffusion method. For IS11, protein
349 concentration was 25 mg mL^{-1}, reservoir solution 0.1 M citric acid, pH 3.5 and 19 % PEG
350 3350). The crystal was cryoprotected by transferring into paratone oil and flash frozen in
351 liquid nitrogen. Diffraction data for the IS11 crystal was collected at 100 K at a Rigaku home
352 source Micromax-007 with R-AXIS IV++ detector and processed using HKL3000 (49). The
353 structure was solved by molecular replacement using Phenix.phaser (50) and a model built by
354 AlphaFold2 (51). Model building and refinement were performed using Phenix.refine and
355 Coot (52). TLS parameterization was utilized for refinement, and *B*-factors were refined as
356 isotropic. Structure geometry and validation were performed using the Phenix Molprobity
357 tools. Data collection and refinement statistics for this structure are summarized in Table S3.

358 **Accession numbers.** SSU rRNA gene sequences were deposited to GenBank as BioProject
359 ID: PRJNA881593. Sequences of IS10-IS12 proteins were deposited to GenBank under
360 accession numbers OL304252, OL304253, and OL304254. The atomic coordinates of IS11
361 have been deposited in the Protein Data Bank (PDB), with accession code 7SPN.

362

363 **RESULTS and DISCUSSION**

364 **Natural microbial communities of terrestrial hydrothermal vents of Ischia and effect of**
365 **polyester enrichments.** To provide insights into the composition of natural microbial
366 communities and thermophilic enzymes of hydrothermal vents of the island of Ischia, four
367 sediment samples were collected from the Cavascura hot spring (samples IS1 and IS2) and
368 from Maronti beach near Sant'Angelo (samples IS3 and IS4) (see Materials and Methods).
369 Both sites represent thermophilic habitats with slightly different environmental conditions:
370 IS1 (pH 7.0, 45 ºC), IS2 (pH 8.5, 55 ºC), IS3 (pH 4.5, 75 ºC), and IS4 (pH 5.0, 85 ºC) (Table
371 S1). From each sample, total DNA was extracted and subjected to barcoded amplicon

sequencing of the V4 region of 16S rRNA gene. Sequence analysis revealed that the IS1 community comprised mainly *Pseudomonas* (17.2 %), class Anaerolineae (Chloroflexi) (12.3%), class Armatimonadota (10.0%), *Elizabethkingia* (phylum Bacteroidota) (9.5%), other Myxococcota (9.1 %), *Sphingobacterium* (order Sphingobacteriales, class Bacteroidia, phylum Bacteroidota) (6.7 %), and class Nitrospirota (6.4%), whereas the IS2 community was dominated by *Caldimonas* (order Burkholderiales, class Gammaproteobacteria) (63.9 %), *Cutibacterium* (order Propionibacteriales, class Actinobacteria) (17.2%), and *Thermus* (phylum Deinococcota) (16 %) (Fig. 1). In contrast, the IS3 community was mainly represented by Bacillales (Firmicutes), namely *Brevibacillus* (48.3%) and *Geobacillus* (42 %), and other Bacilli (4.4 %), whereas IS4 comprised *Sphingobacterium* (Sphingobacteriales, Bacteroidetes) (31.9 %), *Thermobaculum* (Thermobaculales, Chloroflexi) (17.4 %) and *Geobacillus* (10.7 %), followed by *Pseudomonas* (7%) and *Bacillus* (6.1%) (Fig. 1). The observed differences in the taxonomic composition of the Cavascura (IS1 and IS2) and Maronti (IS3 and IS4) samples can be attributed to different environmental conditions (temperature and pH) at the sampling sites.

Using the four sediment samples from two Ischia sites, twelve enrichment cultures were established with different polyester plastics as carbon substrate including PHB, PLA and commercial polyester blend (Table S1). After two weeks of incubation with polyesters, the IS1 enrichment culture showed a drastic increase in the relative abundance of members of the order Burkholderiales within the families Comamonadaceae and Rhodocyclaceae (relative abundance 15.2-35.1 % across the three plastic enrichments), *Fontimonas* (Solimonadaceae, 16.9-27.5%), and *Schleiferia* (order Flavobacteriales, 15.6-34.4%) (Fig. 1). Likewise, IS2 enrichment showed an increase in *Fontimonas* (11-26%), *Schleiferia* (21% in PHB enrichment), whereas the relative content of the *Caldimonas* decreased from 63 % to 5.7 %, in favour of members of other families of the order Burkholderiales, namely Rhodocyclaceae, Hydrogenophilaceae and Comamonadaceae (18-43%) Kapabacteriales (phylum Bacteroidota, 2.9-8%) and Rehaibacterium (order Xanthomonadales, 0.3-9.3 %) (Fig. 1). The enrichment culture with the compostable P3 blend stimulated the growth of Rhodocyclales, as both IS1 and IS2 showed a strong increase in *Thauera* compared to experiments with PHB and PLA (Fig. 1). In the enrichment cultures IS3 and IS4, higher incubation temperature (75°C) selected for thermophilic bacteria, and the nature of polyester used for enrichments influenced the microbial composition (Fig. 1). The PHB enrichment stimulated growth of *Thermus* (Deinococcota), which accounted for 66.7 % (92-fold increase) and 90.9% (1,280-fold increase) of the total reads in IS3 and IS4, respectively, followed by *Geobacillus* and other members of Firmicutes. In contrast, the PLA culture favoured growth of *Geobacillus*, which reached a relative abundance of 95.8% in IS3 (2.3-fold increase) and 91.8% in IS4 (8.6-fold increase), followed by *Thermus* and *Brevibacillus*. Finally, the commercial polyester blend promoted growth of both *Geobacillus* (accounted for 68 % or 1.6-fold increase) and *Thermus* (accounted for 31.5% or 43.8-fold increase) in the IS3 enrichment, whereas the IS4 culture was dominated by Firmicutes, *Geobacillus* (81 %), *Paenibacillus* (11.9%), *Brevibacillus* (5.9 %), and *Thermus* (1.18%). As expected, the Shannon index of microbial diversity (a measure of diversity of species in a community) (Fig. S1) revealed an overall tendency to decrease after incubation with polyester plastics, with the exception of IS2, which also showed low diversity in the native sample with the flattened rarefaction curve (Fig. S1).

Activity-based screening of the hydrothermal metagenome library from Ischia for carboxylesterase activity. After two weeks of incubation with polyesters, total DNA was extracted from the enrichment cultures and combined for the construction of the metagenomic fosmid libraries IS_Lib1 and IS_Lib2. In order to identify carboxylesterases with high-temperature profiles, this library was screened for esterase activity with tributyrin as substrate (for carboxylesterases and lipases) at three temperatures: 37, 50 and 70 °C. Emulsified tributyrin gives a turbid appearance to the plates, and the presence of active metagenomic esterases or lipases is seen as a clear zone around the colony. After screening 3,456 clones from the IS_Libr2 library on tributyrin agar plates, 64 positive hits were identified with 19 positive clones observed at 37 °C, 27 clones at 50 °C, and 18 clones at 70 °C. Furthermore, eight esterase positive clones detected at 50 °C were found to be unique for this temperature, whereas one unique clone was found at 70 °C suggesting that these esterases are mostly active only at elevated temperatures. Following endonuclease digestion profiling and Sanger sequencing analysis, 14 non-redundant fosmids were selected for insert sequencing using the Illumina platform, and fosmid inserts were assembled with an average size of 39 kbp. Sequence analysis revealed 12 putative ORFs encoding predicted hydrolases (including peptidases, carboxylesterases, β-lactamases, serine proteases) homologous to proteins from Chloroflexi and metagenome assembled genome (MAG) affiliated to thermophilic Chloroflexi. From candidate proteins cloned in *E. coli*, three putative carboxylesterases (IS10, IS11, and IS12) were soluble, when expressed in *E. coli* cells, and the presence of carboxylesterase activity in purified proteins was confirmed using tributyrin agarose plates assay (Table 1) and were further selected for detailed biochemical characterisation. Amino acid sequences of IS10 (314 amino acids), IS11 (455 aa), and IS12 (318 aa) showed no presence of recognizable signal peptides. Both IS10 and IS12 belonged to the α/β hydrolase superfamily and had 56.8% sequence identity one to another, whereas IS11 showed no significant sequence similarity to IS10 and IS12 as it was a member of the large family of β-lactamases and penicillin-binding proteins (Table 1). A blastP search of the nrNCBI database revealed that amino acid sequences of IS10 and IS12 were identical to two putative α/β hydrolases from uncultured Chloroflexi bacteria (GenBank accession numbers HEG24678.1 and HHR50377.1, respectively), whereas the IS11 sequence exhibited the highest identity (99.1%) to the putative "class A β-lactamase-related serine hydrolase" HDX58025.1 from uncultured Dehalococcoidia. Interestingly, the top homologous proteins of Ischia esterases were the proteins identified in metagenome from a deep-sea hydrothermal vent (black smoker) in the Mid-Atlantic Ridge (South Atlantic Ocean) (53). The comparison with previously characterised proteins showed the thermostable arylesterase, Are, from *Saccharolobus solfataricus* (UniProt ID B5BLW5, 306 aa) being the top homologue for IS10 (42 % sequence identity), whereas the metagenome-derived esterase Est8 (KP699699, PDB 4YPV, 348 aa) was the top characterised homologue for IS12 (56 % sequence identity) (54,55) (Fig. S2). The IS11 sequence was homologous to penicillin-binding proteins and β-lactamases with low sequence similarity to the CmcPBP from Actinobacteria *Amycolatopsis lactamdurans* (Q06317, 36 % identity) and esterase EstB from *Burkholderia gladioli* (Q9KX40, 32 % identity) (56,57). Domain and multiple sequence alignment confirmed the presence of conserved regions and motifs linked to esterase activity in lipolytic families previously described (Fig. S2 and S3). IS10 and IS12 contained an α/β hydrolase fold (PF07859), displaying the characteristic catalytic triad composed of Ser^{155}, Asp^{250} and His^{281}

463 and the conserved consensus motif G-x-S-x-G around the active site serine (22), clustering
464 together with representatives of family IV (Fig. S2 and S3).

465 The protein IS11 contained a β-lactamase domain (PF00144) and the consensus
466 tetrapeptide S-x-x-K, perfectly conserved among all penicillin-binding enzymes and β-
467 lactamases, surrounding the active serine Ser68. In addition, Lys71 and Tyr160 were also
468 conserved as part of the catalytic triad of family VIII esterases, which groups enzymes with
469 homology to class C β-lactamases and penicillin-binding proteins (Fig. S2 and S3).

470 **Biochemical characterisation of purified metagenomic carboxylesterases using model**
471 **esterase substrates.** The esterase activity of purified proteins (IS10, IS11, IS12) was
472 initially evaluated using model esterase substrates with different chain lengths (C2-C16) at 30
473 ºC (to diminish spontaneous substrate degradation at high temperatures). The proteins were
474 found to be active against several short acyl chain substrates with IS10 and IS11 showing a
475 preference to *p*NP-butyrate, αN-butyrate, and *p*NP-hexanoate, whereas IS12 was most active
476 with *p*NP-acetate and αN-propionate (Fig. 2). All enzymes were active within a broad pH
477 range (pH 6.0-9.0) with maximal activities at pH 9 (Fig. S4a). The purified metagenomic
478 carboxylesterases exhibited saturation kinetics with model esterase substrates at optimal pH
479 9.0 and 30 ºC (Table 2). IS10 appeared to be the most efficient esterase compared to IS11 and
480 IS12, with the highest substrate affinity (lowest K_M) and catalytic efficiency (k_{cat}/K_M) towards
481 the tested model substrates. IS12 showed higher substrate affinity to *p*NP-butyrate and higher
482 activity with *p*NP-acetate than IS11, whereas the latter was more active against *p*NP-butyrate
483 (Table 2).

484 Since the selected carboxylesterases originated from thermophilic environments, we
485 investigated the effect of temperature on the activity (temperature profiles) and
486 thermostability of purified carboxylesterases using *p*-NP-butyrate as substrate (Fig. 3). All
487 enzymes showed considerable activity at 20 ºC, but reaction rates increased 5-10 times at
488 higher temperatures with IS10 showing the highest activity at 60-70 ºC, whereas IS12 was
489 most active at 70ºC-80ºC and IS11 at 80-90 ºC (Fig. 3). The thermostability of purified
490 enzymes was analysed using 20 min preincubation at different temperatures (from 30 to
491 95ºC) followed by esterase assays with *p*NP-butyrate at 30 ºC. IS10 retained 60% activity
492 after preincubation at 50 ºC and showed a complete loss of activity at 80 ºC (Fig. 3). In
493 contrast, both IS11 and IS12 revealed a significant decrease of activity only after 20 min
494 preincubation at 90 ºC and 70 ºC, respectively. After two hours of incubation at 70 ºC, IS12
495 retained 50% of initial activity, but was completely inactivated at 80 ºC (Fig. 4). However,
496 IS11 showed no loss or a small reduction of activity at 70 ºC and 80 ºC, respectively, and
497 required over three hours of incubation at 90ºC for inactivation (Fig. 4). Thus, the
498 metagenomic carboxylesterases from the Ischia hydrothermal vents are the thermophilic
499 enzymes highly active at 70-80 ºC with IS11 and IS12 also showing significant
500 thermostability at temperatures from 60 to 80 ºC. Furthermore, the thermostability of IS11
501 and IS12 was comparable with, or exceeded the, thermostability of other esterases identified
502 in high-temperature environments (41,58-61).

503 Esterase activity of purified metagenomic esterases was inhibited by high concentrations
504 of NaCl (50-67% of remaining activity in the presence of 0.5 M NaCl) with IS11 showing a
505 slightly higher resistance (Fig. S4). Similarly, IS11 retained higher activity in the presence of
506 non-ionic detergents (43% and 53% in the presence of 2% Triton X-100 and Tween 20) (Fig.

S4). With organic solvents, IS10 was inhibited by acetone, acetonitrile, ethanol, and isopropanol (10 %, v/v) (Fig. S5). In contrast, IS11 was more tolerant to these solvents (10-50 %) and was stimulated by 10% ethanol (60% increase) and 30% methanol (84% increase). Furthermore, low concentrations of these solvents (10%, v/v) stimulated esterase activity of IS12 (26-34 % increase), whereas higher concentrations of acetone (50 % v/v) and isopropanol (30% v/v) were inhibiting. Finally, DMSO (10-30 %) stimulated esterase activity of enzymes (20-46 % increase) but was inhibitory to IS10 at 30% (Fig. S5).

Substrate range of purified carboxylesterases. To analyse the substrate range and preference of metagenomic carboxylesterases from the Ischia hydrothermal vents, the purified proteins were examined for the presence of hydrolytic activity against chemically and structurally diverse esters, including alkyl and aryl esters (Materials and Methods). Both IS10 and IS12 revealed a broad substrate range with significant activity against all 44 esters tested ester substrates and the highest activity with phenyl acetate, phenyl propionate, glyceryl tripropionate, tributyrin, and αN-acetate (Table S2). IS12 was also highly active toward vinyl propionate. The broad substrate range of IS10 and IS12 correlates with relatively large effective volumes of their active sites, 650.23 $Å^3$ and 780.5 $Å^3$, respectively (calculated as cavity volume/solvent accessible surface area) (23). These volumes are the largest calculated for prokaryotic esterases experimentally characterised so far, with only CalA lipase (Novozym 735) from the yeast *C. antarctica* having a larger value (23). IS11 had a more restricted substrate range, showing detectable activity against 22 ester substrates of 44 tested with a preference for benzyl (R)-(+)-2-hydroxy-3-phenylpropionate (Table S2). In this study we found this ester being hydrolysed by the three esterases (IS10, IS11, IS12), but preferentially by IS11, suggesting that either the lipocalin domain of IS11 or the hydrophobic and polar residues located at the active site of this esterase (see structural features below) may have a role for the preference of this ester, not only as compared to the other two esterases but also as compared to other esters. The three metagenomic esterases revealed no apparent enantio-preference and hydrolysed both enantiomers of several tested commercially available chiral substrates.

The purified metagenomic esterases were also tested for hydrolytic activity against the T-2 mycotoxin, which contains three ester groups on its side chains. The T-2 and deacetylated HT-2 toxins are members of the large group of trichothecene mycotoxins (over 190 derivatives) containing a tetracyclic ring system (62). Mycotoxins are highly toxic fungal metabolites frequently contaminating food and feed and causing negative effects on human health, animals, and economy (63,64). While physical and chemical methods have been used to detoxify mycotoxins, biological detoxification using enzymes or microbes is more attractive due to specificity, safety, and costs. With T-2 as substrate, both IS10 and IS12 showed high esterase activity based on a pH-shift assay with phenol red (2.3 U/mg and 4.4 U/mg, respectively, at 37ºC and pH 8.0), whereas IS11 was found to be inactive. Hydrolytic activity of IS10 and IS12 against T-2 was confirmed using HPLC, which also revealed the formation of different reaction products (Fig. 5). IS10 produced HT-2 as the main product, whereas HT-2 was present as the minor product in the reaction mixture with IS12, which produced mostly the T-2 triol as the main product (Fig. 5). Since the T-2 triol is known to be less toxic than T-2 and HT-2 (36,65), IS12 might represent a promising candidate for the biodetoxification of T-2 and HT-2.

Since our metagenomic libraries were prepared using enrichment cultures with synthetic polyesters, the purified esterases were also tested for the presence of polyesterase activity.

Although recent studies on biocatalytic depolymerization of synthetic polyesters including PLA and polyethylene terephthalate (PET) have shown the potential of microbial carboxylesterases, there is an urgent need to identify novel robust polyesterases for applications in plastics recycling (35,48,66). The purified esterases were screened for the presence of polyesterase activity using an agarose plate assay with the emulsified PET model substrate, 3PET. These screens revealed the presence of polyesterase activity against 3PET in both IS10 and IS12, as indicated by the formation of a clear zone around the wells with loaded enzymes after incubation at 37 ºC (Fig. 6A). Purified IS11 did not show a visible clearance zone on the 3PET plate, however the *in vitro* assay of hydrolysis of 3PET by IS11 and HPLC analysis of reaction products, showed an increase in MHET, which was the main hydrolysis product while IS10 and IS12 produced BHET as the principal hydrolysis product (Fig. 6B). Furthermore, enzymes exhibited activity toward PLA, with a clear substrate preference toward P(DL)A, over P(L)LA, over P(D)LA (Fig. 6C). To sum up, both IS10 and IS12 exhibited broad substrate profiles and were able to degrade both mycotoxins and polyesters.

Structural studies of metagenomic carboxylesterases. To provide structural insights into the active site and activity of metagenomic carboxylesterases, purified proteins (IS10, IS11, and IS12) were subjected to crystallization trials. IS11 produced diffracting crystals, and its crystal structure was determined by molecular replacement (Table S3, Materials and Methods). The overall structure of IS11 revealed a protein dimer with protomers composed of two structural domains, an N-terminal β-lactamase-like serine hydrolase domain (1-345 aa) connected via a flexible linker (346-358 aa) to a C-terminal lipocalin domain (Fig. 7 and Fig. S6). Protein oligomerization has been suggested to contribute to thermostability of several thermophilic carboxylesterases (e.g. AFEst, PestE, EstE1) (33,61,67). Accordingly, the results of size-exclusion chromatography of purified IS11, as well as IS10 and IS12, suggest that these proteins exist as dimers in solution (Fig. S7).

The serine β-lactamases (classes A, C, and D) are structurally and evolutionary related to penicillin-binding proteins (the targets of β-lactam antibiotics), which also include hydrolytic DD-peptidases (68,69). The overall structure of the IS11 β-lactamase domain is composed of a mostly α-helical (all-α) sub-domain inserted into an α/β/α sandwich (or an α/β sub-domain) (Fig. 7 and 8 and Fig. S6). The α/β/α sandwich sub-domain includes a nine-stranded antiparallel β-sheet flanked by two helices on each side, whereas the mostly helical sub-domain comprises nine α-helices (Fig. 8). The search for structural homologues of IS11 using the Dali server (70) identified numerous β-lactamase-like proteins with low sequence identity including the *Pyrococcus abyssi* peptidase PAB87 (PDB code 2QMI) and *Pseudomonas fluorescens* β-lactamase AmpC (PDB code 2QZ6) as the top structural homologues (Z-score 36.0-40.2, r.m.s.d. 2.1-2.8 Å, sequence identity 22-29%). The two sub-domains form a groove accommodating the catalytic residues including Ser68 (a nucleophile) and Lys71 (a general base accepting the proton from Ser68 O^{γ}) (1st motif S-x-x-K), Tyr160 and Asn162 (2nd motif Y-x-N/S), and His299 (3rd motif H/R/K-T/S/G-G). Accordingly, the IS11 structure revealed the presence of an additional electron density positioned near the side chains of Ser68, Tyr160, and His299, represents an unknown ligand covalently attached to Ser68 (could not be modeled with various components of the protein purification or crystallization solutions) (Fig. 9a). The positioning of these catalytic residues was also conserved in the active sites of the biochemically characterised carboxylesterases with a β-lactamase fold

(family VIII): EstB from *Burkholderia gladioli* and Pab87 from *Pyrococcus abyssi* (71,72), suggesting a common catalytic mechanism with acylation-deacylation. The catalytic cleft of IS11 also contains several hydrophobic and polar residues potentially involved in substrate binding (Asp126, Phe128, Trp158, Asn304, Ile307, Leu309) (Fig. 9).

The C-terminal domain of IS11 represents a typical lipocalin fold with one α-helix and an eight-stranded antiparallel β-barrel containing a hydrophobic core (Fig. 10). Lipocalins are a diverse family of small individual proteins or domains (160-180 aa), which bind various hydrophobic molecules (e.g. fatty acids) in a binding pocket located inside the barrel (73). Although lipocalins are very divergent in their sequences and functions, their structures exhibit remarkable similarity. The lipocalin α-helix of IS11 closes off the top of the β-barrel, whose interior represents a ligand-binding site coated mostly with hydrophobic residues (Fig. 10). In the IS11 protomer, the lipocalin domain covers the β-lactamase domain shielding the catalytic cleft with the extended proline-rich strand (Pro391-Ser409) containing eight Pro residues (Pro391, Pro396, Pro401, Pro402, Pro404, Pro406, Pro407, and Pro408) (Fig. 10). In the thermophilic carboxylesterase Est2 from *Alicyclobacillus acidocaldarius*, the increased number of Pro residues has been suggested to be important for thermostability, because they reduce the flexibility of loops and other structural elements making them more resistant to denaturation (74). The side chains of several residues of the lipocalin domain and proline-rich strand are positioned close to the IS11 active site suggesting that they can be involved in substrate binding (Phe395, Arg397, Lys398, Arg403, Arg449). Typically for all lipocalins, the interior of the IS11 β-barrel is coated by mostly hydrophobic and polar residues (Leu373, Ser374, Ile376, Leu387, Gln389, Leu426, Ser429, Phe444, Phe446, Phe451). Proline-rich sequences are also known to be directly involved or facilitating protein-protein interactions or oligomerization (75). However, the IS11 dimer structure revealed no obvious interactions between the individual lipocalin domains (Fig. S6) suggesting that the lipocalin domain of IS11 participates in substrate binding, rather than in the oligomerization.

High-quality structural models of IS10 and IS12 proteins constructed using the Phyre2 server (Fig. S8) revealed the presence of a core domain with a classical α/β hydrolase fold and an all-helical domain, as well as a serine hydrolase catalytic triad (Ser155, His280, and Asp250 in both proteins) (Fig. S9). The putative catalytic nucleophile Ser155 is located on the classical nucleophilic elbow, a short sharp turn between a β-strand and α-helix. It is located at the bottom of the active site, which is mostly covered by the all-helical lid domain (Fig. S9). Both acyl- and alcohol-binding pockets of IS10 and IS12 include several hydrophobic and polar residues potentially involved in substrate binding (IS10: His81, Trp85, His93, Asn159, Tyr183, Val185, Leu252; IS12: Trp85, Ile87, His93, Asn159, Tyr183, Leu252, Ile279, Val283, Thr284, Leu285) (Fig. S9). Furthermore, the lid domains of both enzymes contain additional hydrophobic residues, which can contribute to substrate binding (IS10: Phe34, Met38, Phe203, Leu204, Met208, Met209, Tyr211; IS12: Phe22, Met34, Tyr195, Leu203, Leu204, Met209, Phe212, Trp213).

CONCLUSION

Present work has demonstrated a high value of high-temperature microbial habitats, particularly of the volcanic island of Ischia (Italy), Terme di Cavascura and Maronti Beach hydrotherms populated by taxonomically diverse microorganisms, as a resource for discovery

of high-temperature active enzymes. As revealed by an in-depth characterization of three metagenomics-derived carboxylesterases (IS10, IS11 and IS12) they were active at temperatures as high as 70-90 ºC and were capable to degradation of bio-based and synthetic polyester plastics. The 3PET was hydrolysed by IS10 and IS12 to predominantly BHET, while IS11 produced MHET as a main product. Interestingly, IS12 further degraded mycotoxin T-2, a common agent causing poisoning the animal feed, to the less toxic T-2 triol. The three wild-type enzymes may readily be applicable in pilot trials in industrial processes relevant to the circular bioeconomy for plastics and/or in the production of toxin free foods and feeds. This study can also serve as a starting point for deepening our knowledge on structural determinants for substrate specificity in carboxylesterases and for rational engineering to further improve their catalytic efficiencies to make them accepting PET oligomers larger than 3PET.

ACKNOWLEDGMENTS

This study was conducted under the auspices of the FuturEnzyme Project funded by the European Union's Horizon 2020 Research and Innovation Programme under Grant Agreement No. 101000327. M.F. and F.J.P. also acknowledge grants PID2020-112758RB-I00 (M.F.), PDC2021-121534-I00 (M.F.), TED2021-130544B-I00 (M.F.) and PID2019-105838RB-C31 (F.J.P.) from the MCIN/AEI/10.13039/501100011033 and the European Union ("NextGenerationEU/PRTR"). M.A.D., T.T.C., R.B., A.N.K., O.V.G., A.F.Y. and P.N.G. thank the support from the European Regional Development Fund (ERDF) through the Welsh Government to the Centre for Environmental Biotechnology (CEB), Project Nr 81280. P.N.G. and A.F.Y. acknowledge the Natural Environment Research Council UK (NERC)-funded Plastic Vectors project NE/S004548/1 and the Sêr Cymru programme partly funded by the ERDF through the Welsh Government for the support of the project BioPOL4Life. We are indebted to Connie Tulloch and Gwion Williams for their technical support.

FIGURE LEGENDS

Fig. 1. The composition of microbial communities of native samples from the Ischia hydrothermal vents (IS1 (green), IS2 (orange), both from Cavascura; IS3 (purple) and IS4 (magenta), both from Maronti Beach) and their enrichment cultures set up with PHB, PLA and polyester blend and incubated for 4 days at 50 °C (IS1-IS2) or 75 °C (IS3-IS4), with consequent transfer into the fresh medium and incubation at same temperatures for 11 days. The relative abundance of barcoded V4-region 16S rRNA gene amplicon reads derived from particular taxa, is reflected in the sizes of circles. For reference, s. the panel in the top left corner.

Fig. 2. Hydrolytic activity of purified IS10 (A), IS11 (B) and IS12 (C) against model esterase substrates. The reaction mixtures contained the indicated *p*-nitrophenyl esters (*p*NP, white bars) and α-naphthyl esters (αN, grey bars) with different acyl chain lengths (reaction temperature 30 ºC, see Materials and Methods for details).

Fig. 3. Activity temperature profiles and thermostability of purified metagenomic carboxylesterases from Ischia. (A) Esterase activity of purified enzymes with *p*NP-butyrate at different temperatures. (B) Thermostability of purified enzymes measured as residual activity after 20 min preincubation at different temperatures. Esterase activity was determined with *p*NP-butyrate as substrate at 30 ºC. "Ctrl" corresponds to the activity measured at 30 ºC without 20 min of pre-incubation.

Fig. 4. Thermoinactivation of purified IS11 (A) and IS12 (B) at different temperatures. Activity data are presented as relative activity from triplicate measurements ± SD. Residual activity was determined with *p*NP-butyrate at 30 ºC.

Fig. 5. Hydrolytic activity of purified IS10 and IS12 against the mycotoxin T-2: HPLC analysis of reaction products. Purified IS10 and IS12 were incubated with T-2 (at 37 ºC and pH 8.0), and reaction products were analysed using HPLC (see Materials and Methods for experimental details).

Fig. 6. Polyesterase activity of metagenomic esterases against PLA and 3PET. (A) plate assay with emulsified 3PET as substrate. The formation of a clear zone around the wells with loaded enzyme indicates the presence of polyesterase activity. Agarose plates (1.5%) containing 0.2 % emulsified 3PET and loaded proteins (50 µg/well) were incubated at 37 ºC and monitored for three days. Porcine liver esterase (PLE), bovine serum albumin (BSA) and elution buffer (EB) were used as a negative, esterase MGS0105 characterised earlier (45) as a positive control. (B) HPLC assay of 3PET hydrolysis products after 16 h of incubation at 30 ºC, elution buffer was used as a negative control (not shown). (C) HPLC analysis of hydrolysis of PLA incubated with metagenomic esterases for 48 hrs at 30 ºC.

Fig. 7. Crystal structure of IS11. (A), Schematic representation of the IS11 domains: the N-terminal β-lactamase related Ser hydrolase domain is coloured cyan with all-helical sub-domain shown in light blue, whereas the C-terminal lipocalin domain in orange. (B), overall fold of the IS11 protomer shown in three views related by 90º rotations. The protein domains are shown as ribbon diagrams with the core domain (β-lactamase) coloured pale cyan, whereas the C-terminal lipocalin domain is coloured light orange. The position of the active site is indicated by the side chains of catalytic Ser68, Lys71, and Tyr160, whereas the protein N- and C-terminal ends are labelled (N and C).

689 **Fig. 8.** Crystal structure of the IS11 β-lactamase and lipocalin domains. (A), The N-terminal
690 β-lactamase-like domain with two sub-domains coloured pale cyan (α/β) and light pink (all-
691 helical). (B), The lipocalin domain. The domains are shown in three views related by 90º
692 rotations with the N- and C-termini labelled (N and C).

693 **Fig. 9.** Close-up view of the IS11 active site. (A), The core domain showing the active site
694 cleft with catalytic residues: motif-1 (Ser68 and Lys71), motif-2 (Tyr160 and Asn162), and
695 motif-3 (His299). The magenta-coloured mesh represents an additional electron density (a
696 2Fo-Fc omit map contoured at 2.5 σ) covalently attached to the Ser68 side chain. (B), The
697 proline-rich loop of the lipocalin domain covering the active site and residues potentially
698 contributing to substrate binding. Protein ribbon diagrams are coloured grey (the β-lactamase
699 domain) and light orange (the lipocalin domain), whereas the side chains of residues are
700 shown as sticks with green and orange carbons, respectively

701 **Fig. 10.** Crystal structure of the IS11 lipocalin domain: ligand binding site and proline-rich
702 loop. The protein ribbon diagram is coloured in grey with the residues of ligand binding
703 pocket shown as sticks with green carbons and labelled.

704

705 **TABLES**

706

707 **Table 1.** Novel carboxylesterases from the Ischia polyester enrichment metagenomes
708 selected for biochemical and structural characterisation in this study.

Protein name	**Fosmid ID**	**Protein length**	**Predicted M.w.**	**Protein superfamily**	**Host organism** (phylum)
IS10	L2B6_15	314 aa	34.3 kDa	α/β hydrolase	Chloroflexi
IS11	L2F9_18	455 aa	49.4 kDa	β-lactamase	Chloroflexi
IS12	L3G23_11	318 aa	33.9 kDa	α/β hydrolase	Chloroflexi

709

710

711

712

713 **Table 2.** Kinetic parameters of purified metagenomic carboxylesterases from the Ischia
714 hydrothermal vents with model esterase substrates[a].

Protein	**Substrate**	K_M **(mM)**	k_{cat} **(s^{-1})**	k_{cat}/K_M **(s^{-1} M^{-1})**
IS10	*p*NP-acetate	0.05 ± 0.01	41.97 ± 1.79	7.9 x 10^5
	*p*NP-butyrate	0.06 ± 0.01	66.21 ± 3.24	1.2 x 10^6
	*p*NP-hexanoate	0.04 ± 0.01	86.79 ± 3.06	2.0 x 10^6
	αN-propionate	0.06 ± 0.02	31.20 ± 1.93	5.0 x 10^5
	αN-butyrate	0.12 + 0.04	58.60 ± 5.89	4.9 x 10^5
IS11	*p*NP-acetate	0.53 ± 0.31	1.60 ± 0.30	3.0 x 10^3
	*p*NP-butyrate	0.20 ± 0.02	68.81 ± 1.37	3.5 x 10^5
	*p*NP-hexanoate	0.08 ± 0.02	40.28 ± 1.39	5.3 x 10^5
	αN-butyrate	0.09 ± 0.02	5.93 ± 0.49	6.9 x 10^4
IS12	*p*NP-acetate	0.22 ± 0.05	57.10 ± 3.78	2.6 x 10^5
	*p*NP-butyrate	0.08 ± 0.01	8.77 ± 0.29	1.1 x 10^5
	*p*NP-hexanoate	0.09 ± 0.01	19.05 ± 0.50	2.1 x 10^5
	αN-propionate	0.69 ± 0.19	39.45 ± 3.7	5.7 x 10^4

715 [a] Reaction conditions were as indicated in Materials and Methods (pH 9.0, 30ºC). Results are
716 mean ± SD of three independent experiments. αN = α-naphthyl, *p*NP = *p*-nitrophenyl.

717

718

719

720

721

722

723

724

725

726

727 **REFERENCES**

728 1. Kyrpides NC, Hugenholtz P, Eisen JA, Woyke T, Goker M, Parker CT, Amann R,
729 Beck BJ, Chain PS, Chun J, Colwell RR, Danchin A, Dawyndt P, Dedeurwaerdere T,
730 DeLong EF, Detter JC, De Vos P, Donohue TJ, Dong XZ, Ehrlich DS, Fraser C, Gibbs R,
731 Gilbert J, Gilna P, Glockner FO, Jansson JK, Keasling JD, Knight R, Labeda D, Lapidus A,
732 Lee JS, Li WJ, Ma J, Markowitz V, Moore ER, Morrison M, Meyer F, Nelson KE, Ohkuma
733 M, Ouzounis CA, Pace N, Parkhill J, Qin N, Rossello-Mora R, Sikorski J, Smith D, Sogin M,
734 Steven R, Stingl U, Suzuki K, Taylor D, Tiedje JM, Tindall, B, Wagner M, Weinstock G,
735 Weissenbach J, White O, Wang J, Zhang L, Zhou YG, Field D, Whitman WB, Garrity GM,
736 Klenk HP. 2014. Genomic encyclopedia of bacteria and archaea: sequencing a myriad of type
737 strains. PLoS Biol 12:e1001920

738 2. Yarza P, Yilmaz P, Pruesse E, Glockner FO, Ludwig W, Schleifer KH, Whitman WB,
739 Euzeby J, Amann R, Rossello-Mora R. 2014. Uniting the classification of cultured and
740 uncultured bacteria and archaea using 16S rRNA gene sequences. Nat Rev Microbiol 12:635-
741 645

742 3. Rappe MS, Giovannoni SJ. 2003. The uncultured microbial majority. Annu Rev
743 Microbiol 57:369-394

744 4. Torsvik V, Goksoyr J, Daae FL. 1990. High diversity in DNA of soil bacteria. Appl
745 Environ Microbiol 56:782-787

746 5. Handelsman J. 2004. Metagenomics: application of genomics to uncultured
747 microorganisms. Microbiol Mol Biol Rev 68:669-685

748 6. Ferrer M, Golyshina O, Beloqui A, Golyshin PN. 2007. Mining enzymes from
749 extreme environments. Curr Opin Microbiol 10:207-214

750 7. Uchiyama T, Miyazaki K. 2009. Functional metagenomics for enzyme discovery:
751 challenges to efficient screening. Curr Opin Biotechnol 20:616-622

752 8. Turnbaugh PJ, Gordon JI. 2008. An invitation to the marriage of metagenomics and
753 metabolomics. Cell 134:708-713

754 9. Venter JC, Remington K, Heidelberg JF, Halpern AL, Rusch D, Eisen JA, Wu D,
755 Paulsen I, Nelson KE, Nelson W, Fouts DE, Levy S, Knap AH, Lomas MW, Nealson K,
756 White O, Peterson J, Hoffman J, Parsons R, Baden-Tillson H, Pfannkoch C, Rogers YH,
757 Smith HO. 2004. Environmental genome shotgun sequencing of the Sargasso Sea. Science
758 304:66-74

759 10. Rusch DB, Halpern AL, Sutton G, Heidelberg KB, Williamson S, Yooseph S, Wu D,
760 Eisen JA, Hoffman JM, Remington K, Beeson K, Tran B, Smith H, Baden-Tillson H, Stewart
761 C, Thorpe J, Freeman J, Andrews-Pfannkoch C, Venter JE, Li K, Kravitz S, Heidelberg JF,
762 Utterback T, Rogers YH, Falcón LI, Souza V, Bonilla-Rosso G, Eguiarte LE, Karl DM,

763 Sathyendranath S, Platt T, Bermingham E, Gallardo V, Tamayo-Castillo G, Ferrari MR,
764 Strausberg RL, Nealson K, Friedman R, Frazier M, Venter JC. 2007. The Sorcerer II Global
765 Ocean Sampling expedition: northwest Atlantic through eastern tropical Pacific. PLoS Biol
766 5:e77

767 11. Yooseph S, Sutton G, Rusch DB, Halpern AL, Williamson SJ, Remington K, Eisen
768 JA, Heidelberg KB, Manning G, Li W, Jaroszewski L, Cieplak P, Miller CS, Li H,
769 Mashiyama ST, Joachimiak MP, van Belle C, Chandonia JM, Soergel DA, Zhai Y, Natarajan
770 K, Lee S, Raphael BJ, Bafna V, Friedman R, Brenner SE, Godzik A, Eisenberg D, Dixon JE,
771 Taylor SS, Strausberg RL, Frazier M, Venter JC. 2007. The Sorcerer II Global Ocean
772 Sampling expedition: expanding the universe of protein families. PLoS Biol 5:e16

773 12. Qin J, Li R, Raes J, Arumugam M, Burgdorf KS, Manichanh C, Nielsen T, Pons N,
774 Levenez F, Yamada T, Mende DR, Li J, Xu J, Li S, Li D, Cao J, Wang B, Liang H, Zheng H,
775 Xie Y, Tap J, Lepage P, Bertalan M, Batto JM, Hansen T, Le Paslier D, Linneberg A, Nielsen
776 HB, Pelletier E, Renault P, Sicheritz-Ponten T, Turner K, Zhu H, Yu C, Li S, Jian M, Zhou
777 Y, Li Y, Zhang X, Li S, Qin N, Yang H, Wang J, Brunak S, Doré J, Guarner F, Kristiansen
778 K, Pedersen O, Parkhill J, Weissenbach J; MetaHIT Consortium, Bork P, Ehrlich SD, Wang
779 J. 2010. A human gut microbial gene catalogue established by metagenomic sequencing.
780 Nature 464:59-65

781 13. Hess M, Sczyrba A, Egan R, Kim TW, Chokhawala H, Schroth G, Luo S, Clark DS,
782 Chen F, Zhang T, Mackie RI, Pennacchio LA, Tringe SG, Visel A, Woyke T, Wang Z, Rubin
783 EM. 2011. Metagenomic discovery of biomass-degrading genes and genomes from cow
784 rumen. Science 331:463-467

785 14. Ferrer M, Martínez-Martínez M, Bargiela R, Streit WR, Golyshina OV, Golyshin PN.
786 2016. Estimating the success of enzyme bioprospecting through metagenomics: current status
787 and future trends. Microb Biotechnol 9:22-34

788 15. Levitt M. 2009. Nature of the protein universe. Proc Natl Acad Sci U S A 106:11079-
789 11084

790 16. Godzik A. 2011. Metagenomics and the protein universe. Curr Opin Struct Biol
791 21:398-403

792 17. Dinsdale EA, Edwards RA, Hall D, Angly F, Breitbart M, Brulc JM, Furlan M,
793 Desnues C, Haynes M, Li L, McDaniel L, Moran MA, Nelson KE, Nilsson C, Olson R, Paul
794 J, Brito BR, Ruan Y, Swan BK, Stevens R, Valentine DL, Thurber RV, Wegley L, White
795 BA, Rohwer F. 2008. Functional metagenomic profiling of nine biomes. Nature 452:629-632

796 18. Rondon MR, August PR, Bettermann AD, Brady SF, Grossman TH, Liles MR,
797 Loiacono KA, Lynch BA, MacNeil IA, Minor C, Tiong CL, Gilman M, Osburne MS, Clardy
798 J, Handelsman J, Goodman RM. 2000. Cloning the soil metagenome: a strategy for accessing
799 the genetic and functional diversity of uncultured microorganisms. Appl Environ Microbiol
800 66:2541-2547

801 19. Simon C, Daniel R. 2011. Metagenomic analyses: past and future trends. Appl
802 Environ Microbiol 77:1153-1161

803 20. Robertson DE, Chaplin JA, DeSantis G, Podar M, Madden M, Chi E, Richardson T,
804 Milan A, Miller M, Weiner DP, Wong K, McQuaid J, Farwell B, Preston LA, Tan X, Snead
805 MA, Keller M, Mathur E, Kretz PL, Burk MJ, Short JM. 2004. Exploring nitrilase sequence
806 space for enantioselective catalysis. Appl Environ Microbiol 70:2429-2436

807 21. Lorenz P, Eck J. 2005. Metagenomics and industrial applications. Nat Rev Microbiol
808 3:510-516

809 22. Bornscheuer UT. 2002. Microbial carboxyl esterases: classification, properties and
810 application in biocatalysis. FEMS Microbiol Rev 26:73-81

811 23. Martínez-Martínez M, Coscolín C, Santiago G, Chow J, Stogios PJ, Bargiela R,
812 Gertler C, Navarro-Fernández J, Bollinger A, Thies S, Méndez-García C, Popovic A, Brown
813 G, Chernikova TN, García-Moyano A, Bjerga GEK, Pérez-García P, Hai T, Del Pozo MV,
814 Stokke R, Steen IH, Cui H, Xu X, Nocek BP, Alcaide M, Distaso M, Mesa V, Peláez AI,
815 Sánchez J, Buchholz PCF, Pleiss J, Fernández-Guerra A, Glöckner FO, Golyshina OV,
816 Yakimov MM, Savchenko A, Jaeger KE, Yakunin AF, Streit WR, Golyshin PN, Guallar V,
817 Ferrer M, The Inmare Consortium. 2018. Determinants and prediction of esterase substrate
818 promiscuity patterns. ACS Chem Biol 13:225-234

819 24. Arpigny JL, Jaeger KE. 1999. Bacterial lipolytic enzymes: classification and
820 properties. Biochem J 343(Pt 1):177-183

821 25. Lenfant N, Hotelier T, Velluet E, Bourne Y, Marchot P, Chatonnet A. 2013.
822 ESTHER, the database of the alpha/beta-hydrolase fold superfamily of proteins: tools to
823 explore diversity of functions. Nucleic Acids Res 41:D423-429

824 26. Littlechild JA. 2017. Improving the 'tool box' for robust industrial enzymes. J Ind
825 Microbiol Biotechnol 44:711-720

826 27. Popovic A, Hai T, Tchigvintsev A, Hajighasemi M, Nocek B, Khusnutdinova AN,
827 Brown G, Glinos J, Flick R, Skarina T, Chernikova TN, Yim V, Brüls T, Paslier DL,
828 Yakimov MM, Joachimiak A, Ferrer M, Golyshina OV, Savchenko A, Golyshin PN,
829 Yakunin AF. 2017. Activity screening of environmental metagenomic libraries reveals novel
830 carboxylesterase families. Sci Rep 7:44103

831 28. Pellis A, Cantone S, Ebert C, Gardossi L. 2018. Evolving biocatalysis to meet
832 bioeconomy challenges and opportunities. N Biotechnol 40:154-169

833 29. Antranikian G, Streit WR. 2022. Microorganisms harbor keys to a circular
834 bioeconomy making them useful tools in fighting plastic pollution and rising CO2 levels.
835 Extremophiles 26:10

836 30. Kruger A, Schafers C, Schroder C, Antranikian G. 2018. Towards a sustainable
837 biobased industry - Highlighting the impact of extremophiles. N Biotechnol 40:144-153

838 31. Atomi H. 2005. Recent progress towards the application of hyperthermophiles and
839 their enzymes. Curr Opin Chem Biol 9:166-173

840 32. Littlechild JA. 2015. Archaeal enzymes and applications in industrial biocatalysts.
841 Archaea 2015:147671

842 33. Vieille C, Zeikus GJ. 2001. Hyperthermophilic enzymes: sources, uses, and molecular
843 mechanisms for thermostability. Microbiol Mol Biol Rev 65:1-43

844 34. Alcaide M, Stogios PJ, Lafraya Á, Tchigvintsev A, Flick R, Bargiela R, Chernikova
845 TN, Reva ON, Hai T, Leggewie CC, Katzke N, La Cono V, Matesanz R, Jebbar M, Jaeger
846 KE, Yakimov MM, Yakunin AF, Golyshin PN, Golyshina OV, Savchenko A, Ferrer M;
847 MAMBA Consortium. 2015. Pressure adaptation is linked to thermal adaptation in salt-
848 saturated marine habitats. Environ Microbiol 17:332-345

849 35. Wei R, von Haugwitz G, Pfaff L, Mican J, Badenhorst CPS, Liu W, Weber G, Austin
850 HP, Bednar D, Damborsky J, Bornscheuer UT. 2022. Mechanism-based design of efficient
851 PET hydrolases. ACS Catalysis 12:3382-3396

852 36. Heinl S, Hartinger D, Thamhesl M, Vekiru E, Krska R, Schatzmayr G, Moll WD,
853 Grabherr R. 2010. Degradation of fumonisin B1, by the consecutive action of two bacterial
854 enzymes. J Biotechnol 145: 120–129

855 37. Rizzo C, Arcadi E, Calogero R, Sciutteri V, Consoli P, Esposito V, Canese S,
856 Andaloro F, Romeo T. 2022. Ecological and biotechnological relevance of Mediterranean
857 hydrothermal vent systems. Minerals 12:251

858 38. Fadrosh DW, Ma B, Gajer P, Sengamalay N, Ott S, Brotman RM, Ravel J. 2014. An
859 improved dual-indexing approach for multiplexed 16S rRNA gene sequencing on the
860 Illumina MiSeq platform. Microbiome 2:6

861 39. Distaso MA, Bargiela R, Brailsford FL, Williams GB, Wright S, Lunev EA,
862 Toshchakov SV, Yakimov MM, Jones DL, Golyshin PN, Golyshina OV. 2020 High
863 representation of archaea across all depths in oxic and low-pH sediment layers underlying an
864 acidic stream. Front Microbiol 11:2871.

865 40. R Core Team. 2020. R: A language and environment for statistical computing. R
866 Foundation for Statistical Computing, Vienna, Austria. www.R-project.org/.

867 41. Placido A, Hai T, Ferrer M, Chernikova TN, Distaso M, Armstrong D, Yakunin AF,
868 Toshchakov SV, Yakimov MM, Kublanov IV, Golyshina OV, Pesole G, Ceci LR, Golyshin
869 PN. 2015. Diversity of hydrolases from hydrothermal vent sediments of the Levante Bay,
870 Vulcano Island Aeolian archipelago identified by activity-based metagenomics and
871 biochemical characterization of new esterases and an arabinopyranosidase. Appl Microbiol
872 Biotechnol 99:10031-10046

873 42. Zhu W, Lomsadze A, Borodovsky M. 2010. Ab initio gene identification in
874 metagenomic sequences. Nucleic Acids Res 38:e132

875 43. Altschul SF, Madden TL, Schaffer AA, Zhang J, Zhang Z, Miller W, Lipman DJ.
876 1997. Gapped BLAST and PSI-BLAST: a new generation of protein database search
877 programs. Nucleic Acids Res 25:3389-3402

878 44. Edgar RC. 2004. MUSCLE: multiple sequence alignment with high accuracy and
879 high throughput. Nucleic Acids Res 32:1792-1797

880 45. Kumar S, Stecher G, Li M, Knyaz C, Tamura K. 2018. MEGA X: Molecular
881 evolutionary genetics analysis across computing platforms. Mol Biol Evol 35:1547-1549

882 46. Tchigvintsev A, Tran H, Popovic A, Kovacic F, Brown G, Flick R, Hajighasemi M,
883 Egorova O, Somody JC, Tchigvintsev D, Khusnutdinova A, Chernikova TN, Golyshina OV,
884 Yakimov MM, Savchenko A, Golyshin PN, Jaeger KE, Yakunin AF. 2015. The environment
885 shapes microbial enzymes: five cold-active and salt-resistant carboxylesterases from marine
886 metagenomes. Appl Microbiol Biotechnol 99:2165-2178

887 47. Guinta CI, Cea-Rama I, Alonso S, Briand ML, Bargiela R, Coscolin C, Corvini P,
888 Ferrer M, Sanz-Aparicio J, Shahgaldian P. 2020. Tuning the properties of natural
889 promiscuous enzymes by engineering their nano-environment. ACS Nano 14:17652-17664

890 48. Hajighasemi M, Tchigvintsev A, Nocek B, Flick R, Popovic A, Hai T, Khusnutdinova
891 AN, Brown G, Xu X, Cui H, Anstett J, Chernikova TN, Brüls T, Le Paslier D, Yakimov MM,
892 Joachimiak A, Golyshina OV, Savchenko A, Golyshin PN, Edwards EA, Yakunin AF. 2018.
893 Screening and Characterization of Novel Polyesterases from Environmental Metagenomes
894 with High Hydrolytic Activity against Synthetic Polyesters. Environ Sci Technol 52:12388-
895 12401

896 49. Minor W, Cymborowski M, Otwinowski Z, Chruszcz M. 2006. HKL-3000: the
897 integration of data reduction and structure solution--from diffraction images to an initial
898 model in minutes. Acta Crystallogr D Biol Crystallogr 62:859-866

899 50. Liebschner D, Afonine PV, Baker ML, Bunkóczi G, Chen VB, Croll TI, Hintze B,
900 Hung LW, Jain S, McCoy AJ, Moriarty NW, Oeffner RD, Poon BK, Prisant MG, Read RJ,
901 Richardson JS, Richardson DC, Sammito MD, Sobolev OV, Stockwell DH, Terwilliger TC,
902 Urzhumtsev AG, Videau LL, Williams CJ, Adams PD.2019 Macromolecular structure
903 determination using X-rays, neutrons and electrons: recent developments in Phenix. Acta
904 Crystallogr D Struct Biol 75:861-877

905 51. Jumper J, Evans R, Pritzel A, Green T, Figurnov M, Ronneberger O,
906 Tunyasuvunakool K, Bates R, Žídek A, Potapenko A, Bridgland A, Meyer C, Kohl SAA,
907 Ballard AJ, Cowie A, Romera-Paredes B, Nikolov S, Jain R, Adler J, Back T, Petersen S,
908 Reiman D, Clancy E, Zielinski M, Steinegger M, Pacholska M, Berghammer T, Bodenstein
909 S, Silver D, Vinyals O, Senior AW, Kavukcuoglu K, Kohli P, Hassabis D. 2021 Highly
910 accurate protein structure prediction with AlphaFold. Nature 596:583-589

911 52. Emsley P, Cowtan K. 2004. Coot: model-building tools for molecular graphics. Acta
912 Crystallogr D Biol Crystallogr 60:2126-2132

913 53. Zhou Z, Liu Y, Xu W, Pan J, Luo ZH, Li M. 2020. Genome- and Community-Level
914 Interaction Insights into Carbon Utilization and Element Cycling Functions of
915 Hydrothermarchaeota in Hydrothermal Sediment. mSystems 5:e00795-19

916 54. Park YJ, Yoon SJ, Lee HB. 2008. A novel thermostable arylesterase from the
917 archaeon Sulfolobus solfataricus P1: purification, characterization, and expression. J
918 Bacteriol 190:8086-8095

919 55. Pereira MR, Maester TC, Mercaldi GF, de Macedo Lemos EG, Hyvonen M, Balan A.
920 2017. From a metagenomic source to a high-resolution structure of a novel alkaline esterase.
921 Appl Microbiol Biotechnol 101:4935-4949

56. Coque JJ, Liras P, Martin JF. 1993. Genes for a beta-lactamase, a penicillin-binding protein and a transmembrane protein are clustered with the cephamycin biosynthetic genes in Nocardia lactamdurans. EMBO J 12:631-639

57. Petersen EI, Valinger G, Solkner B, Stubenrauch G, Schwab H. 2001. A novel esterase from Burkholderia gladioli which shows high deacetylation activity on cephalosporins is related to beta-lactamases and DD-peptidases. J Biotechnol 89:11-25

58. Lewin A, Strand T, Haugen T, Klinkenberg G, Kotlar H, Valla S., Drablos F, Wentze, A. 2016. Discovery and characterization of a thermostable esterase from an oil reservoir metagenome. Adv Enzyme Res 4:68-86

59. Leis B, Angelov A, Mientus M, Li H, Pham VT, Lauinger B, Bongen P, Pietruszka J, Goncalves LG, Santos H, Liebl W. 2015. Identification of novel esterase-active enzymes from hot environments by use of the host bacterium *Thermus thermophilus*. Front Microbiol 6:275

60. Miguel-Ruano V, Rivera I, Rajkovic J, Knapik K, Torrado A, Otero JM, Beneventi E, Becerra M, Sánchez-Costa M, Hidalgo A, Berenguer J, González-Siso MI, Cruces J, Rúa ML, Hermoso JA. 2021. Biochemical and structural characterization of a novel thermophilic esterase EstD11 provide catalytic insights for the HSL family. Comput Struct Biotechnol J 19:1214-1232

61. Sayer C, Szabo Z, Isupov MN, Ingham C, Littlechild JA. 2015. The structure of a novel thermophilic esterase from the Planctomycetes species, *Thermogutta terrifontis* reveals an open active site due to a minimal 'cap' domain. Front Microbiol 6:1294

62. Loi M, Fanell, F, Liuzzi VC, Logrieco AF, Mule G. 2017. Mycotoxin Biotransformation by native and commercial enzymes: Present and future perspectives. Toxins Basel 9:111

63. Liu L, Xie M, We, D. 2022. Biological Detoxification of Mycotoxins: Current Status and Future Advances. Int J Mol Sci 23:1064

64. Lyagin I, and Efremenko E. 2019. Enzymes for detoxification of various mycotoxins: origins and mechanisms of catalytic action. Molecules 24:2362

65. McCormick SP, Price NP, Kurtzman CP 2012. Glucosylation and other biotransformations of T-2 toxin by yeasts of the trichomonascus clade. Appl Environ Microbiol 78:8694-8702

66. Tournier V, Topham CM, Gilles A, David B, Folgoas C, Moya-Leclair E, Kamionka E, Desrousseaux ML, Texier H, Gavalda S, Cot M, Guémard E, Dalibey M, Nomme J, Cioci G, Barbe S, Chateau M, André I, Duquesne S, Marty A. 2020. An engineered PET depolymerase to break down and recycle plastic bottles. Nature 580:216-219.

67. Palm GJ, Fernández-Álvaro E, Bogdanović X, Bartsch S, Sczodrok J, Singh RK, Böttcher D, Atomi H, Bornscheuer UT, Hinrichs W. 2011. The crystal structure of an esterase from the hyperthermophilic microorganism Pyrobaculum calidifontis VA1 explains its enantioselectivity. Appl Microbiol Biotechnol 91:1061-1072

68. Sauvage E, Kerff F, Terrak M, Ayala JA, Charlier P. 2008. The penicillin-binding proteins: structure and role in peptidoglycan biosynthesis. FEMS Microbiol Rev 32:234-258

69. Lee D, Das S, Dawson NL, Dobrijevic D, Ward J, Orengo C. 2016. Novel computational protocols for functionally classifying and characterising serine beta-lactamases. PLoS Comput Biol 12:e1004926

70. Holm L. 2022. Dali server: structural unification of protein families. Nucleic Acids Res 50:W210-W215

71. Wagner UG, Petersen EI, Schwab H, Kratky C. 2002. EstB from *Burkholderia gladioli*: a novel esterase with a beta-lactamase fold reveals steric factors to discriminate between esterolytic and beta-lactam cleaving activity. Protein Sci 11:467-478

72. Delfosse V, Girard E, Birck C, Delmarcelle M, Delarue M, Poch O, Schultz O, Mayer C. 2009. Structure of the archaeal pab87 peptidase reveals a novel self-compartmentalizing protease family. PLoS One 4:e4712

73. Flower DR, North AC, Sansom CE. 2000. The lipocalin protein family: structural and sequence overview. Biochim Biophys Acta 1482:9-24

74. De Simone G, Galdiero S, Manco G, Lang D, Rossi M, Pedone C. 2000. A snapshot of a transition state analogue of a novel thermophilic esterase belonging to the subfamily of mammalian hormone-sensitive lipase. J Mol Biol 303:761-771

75. Kay BK, Williamson MP, Sudol M. 2000. The importance of being proline: the interaction of proline-rich motifs in signaling proteins with their cognate domains. FASEB J 14:231-241

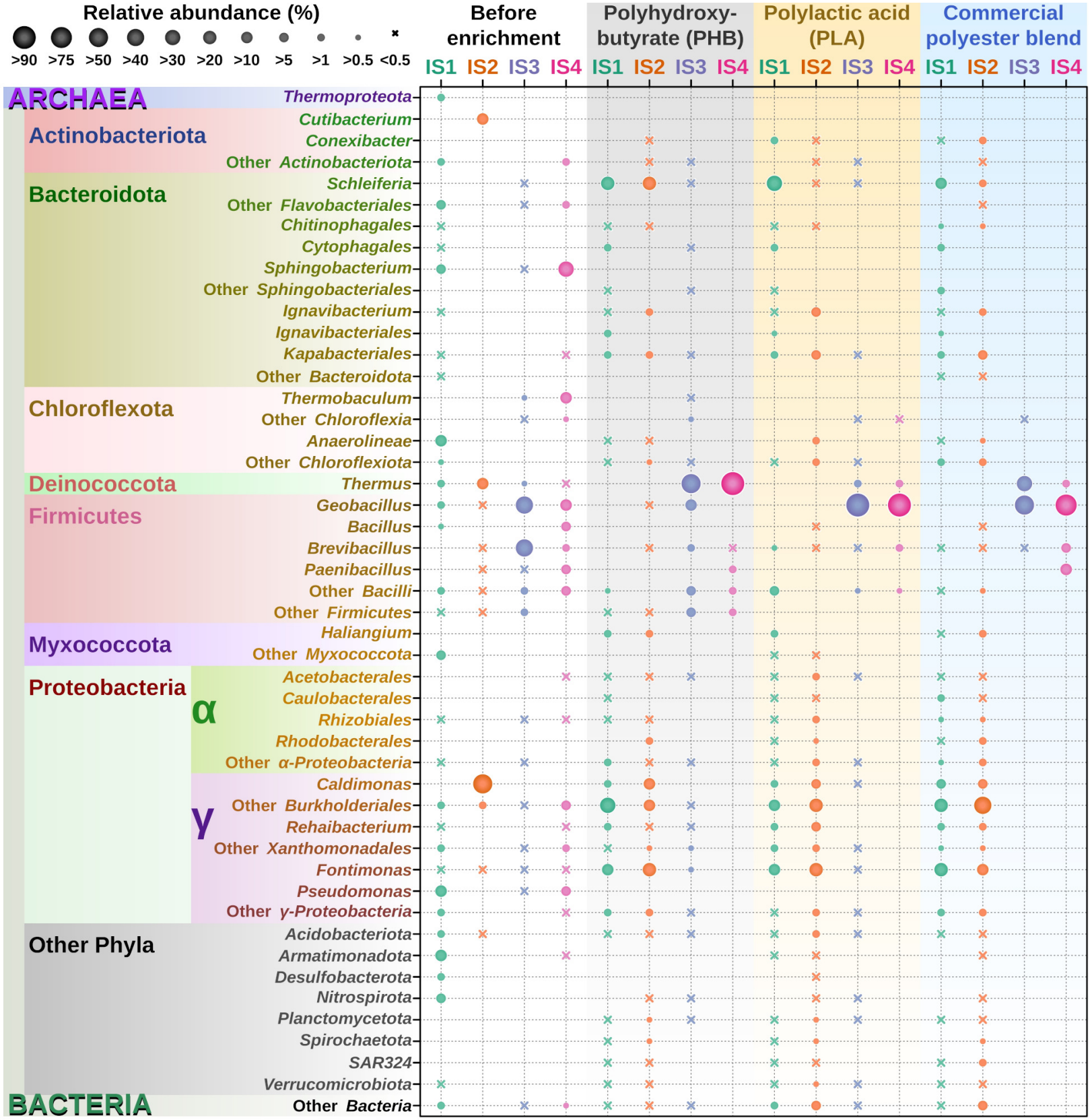
Relative abundance (%)
>90 >75 >50 >40 >30 >20 >10 >5 >1 >0.5 <0.5
Before enrichment
Polyhydroxy-butyrate (PHB)
Polylactic acid (PLA)
Commercial polyester blend
IS1 IS2 IS3 IS4
ARCHAEA
Thermoproteota
Actinobacteriota
Cutibacterium
Conexibacter
Other Actinobacteriota
Bacteroidota
Schleiferia
Other Flavobacteriales
Chitinophagales
Cytophagales
Sphingobacterium
Other Sphingobacteriales
Ignavibacterium
Ignavibacteriales
Kapabacteriales
Other Bacteroidota
Chloroflexota
Thermobaculum
Other Chloroflexia
Anaerolineae
Other Chloroflexiota
Deinococcota
Thermus
Firmicutes
Geobacillus
Bacillus
Brevibacillus
Paenibacillus
Other Bacilli
Other Firmicutes
Myxococcota
Haliangium
Other Myxococcota
Proteobacteria
α
Acetobacterales
Caulobacterales
Rhizobiales
Rhodobacterales
Other α-Proteobacteria
γ
Caldimonas
Other Burkholderiales
Rehaibacterium
Other Xanthomonadales
Fontimonas
Pseudomonas
Other γ-Proteobacteria
Other Phyla
Acidobacteriota
Armatimonadota
Desulfobacterota
Nitrospirota
Planctomycetota
Spirochaetota
SAR324
Verrucomicrobiota
BACTERIA
Other Bacteria

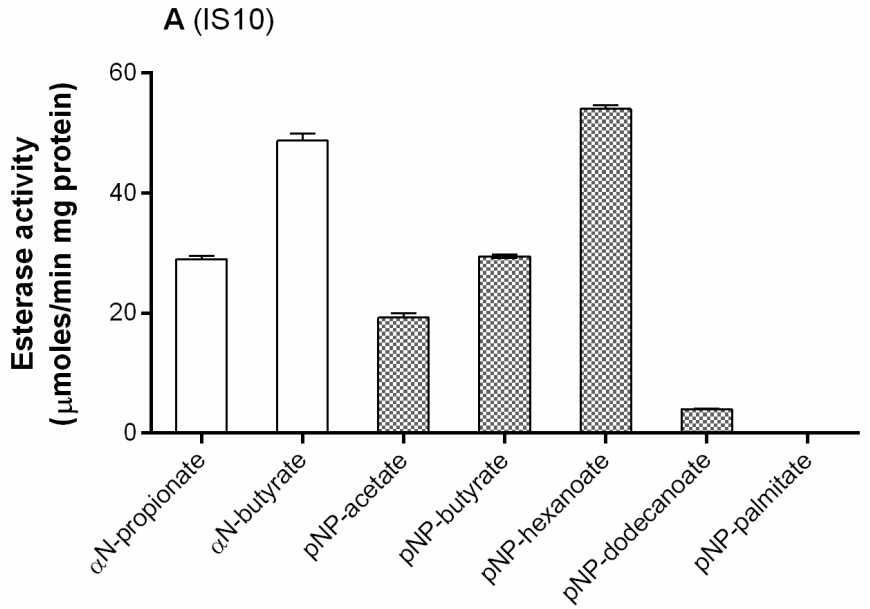
A (IS10)
Esterase activity
(μmoles/min mg protein)
60
40
20
0
αN-propionate
αN-butyrate
pNP-acetate
pNP-butyrate
pNP-hexanoate
pNP-dodecanoate
pNP-palmitate

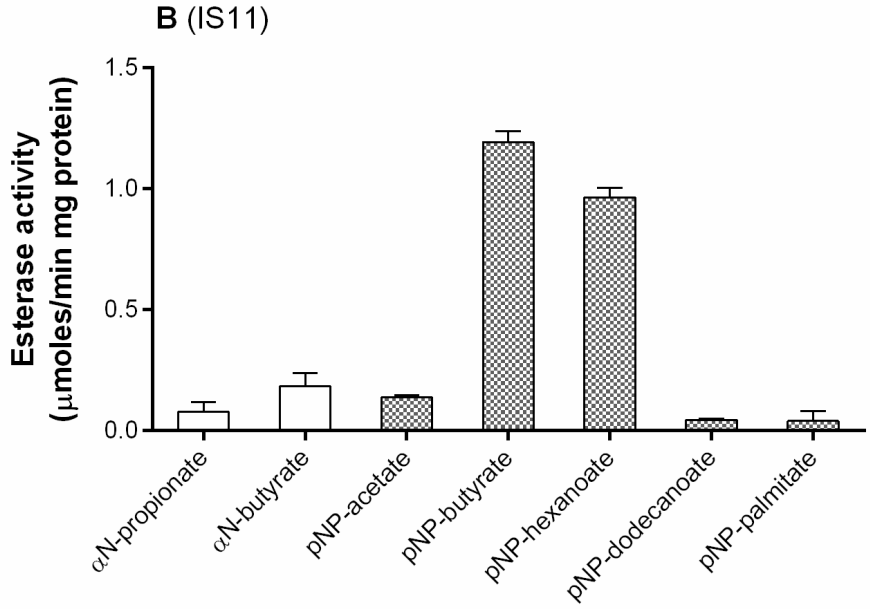
B (IS11)
Esterase activity
(μmoles/min mg protein)
1.5
1.0
0.5
0.0
αN-propionate
αN-butyrate
pNP-acetate
pNP-butyrate
pNP-hexanoate
pNP-dodecanoate
pNP-palmitate

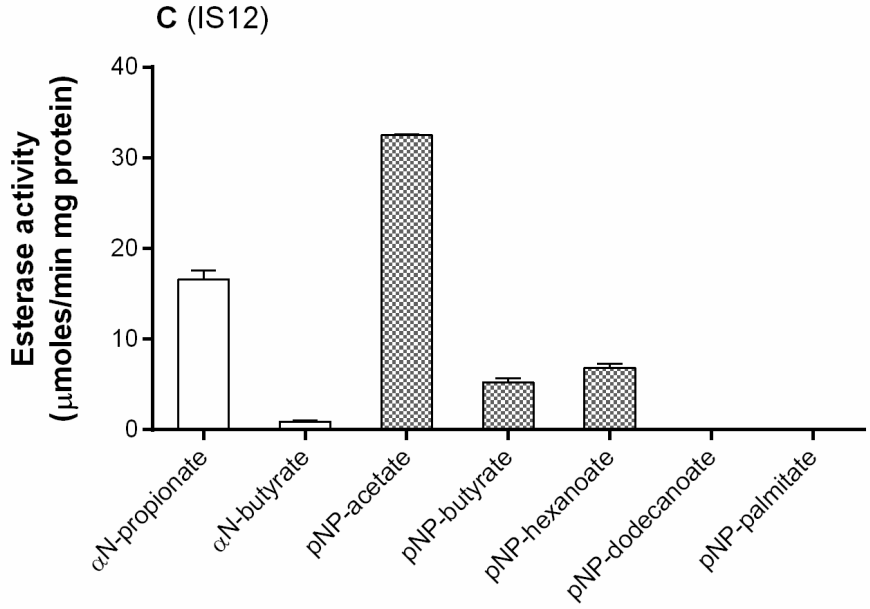
C (IS12)
Esterase activity
(μmoles/min mg protein)
40
30
20
10
0
αN-propionate
αN-butyrate
pNP-acetate
pNP-butyrate
pNP-hexanoate
pNP-dodecanoate
pNP-palmitate

A

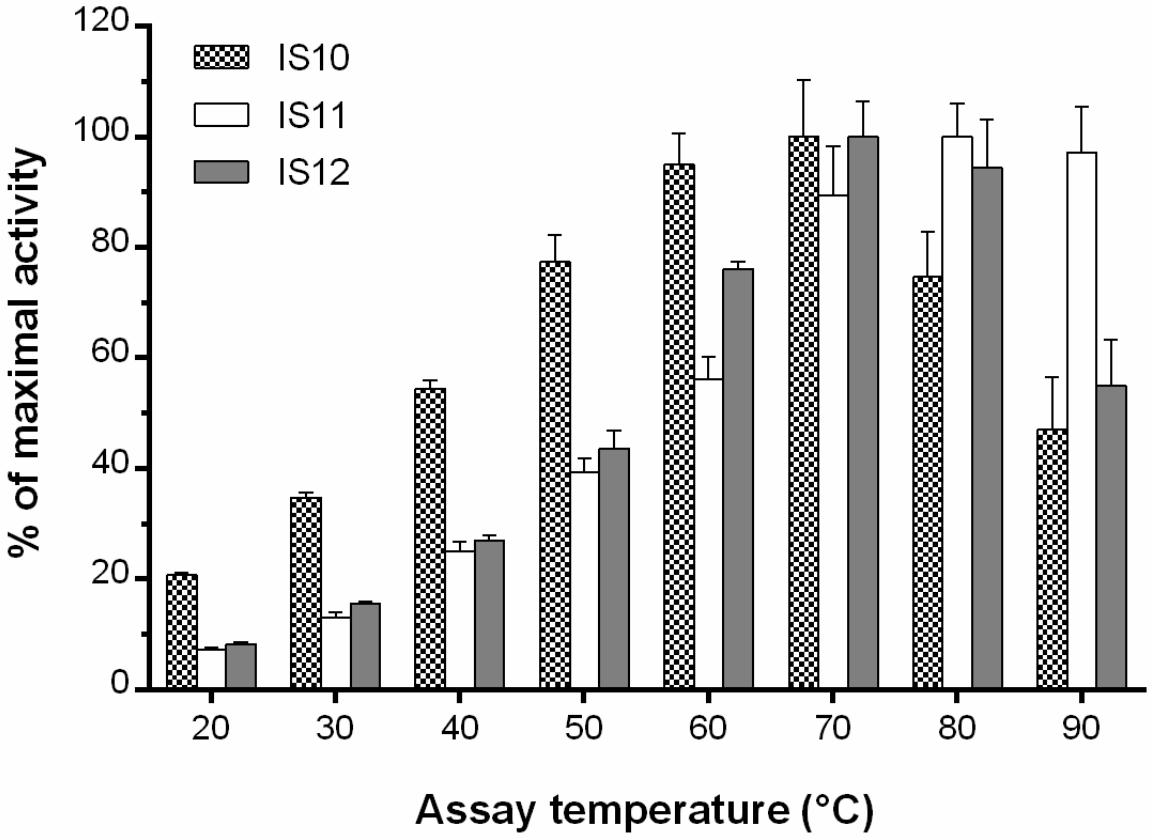
IS10
IS11
IS12
% of maximal activity
0
20
40
60
80
100
120
20
30
40
50
60
70
80
90
Assay temperature (°C)

B

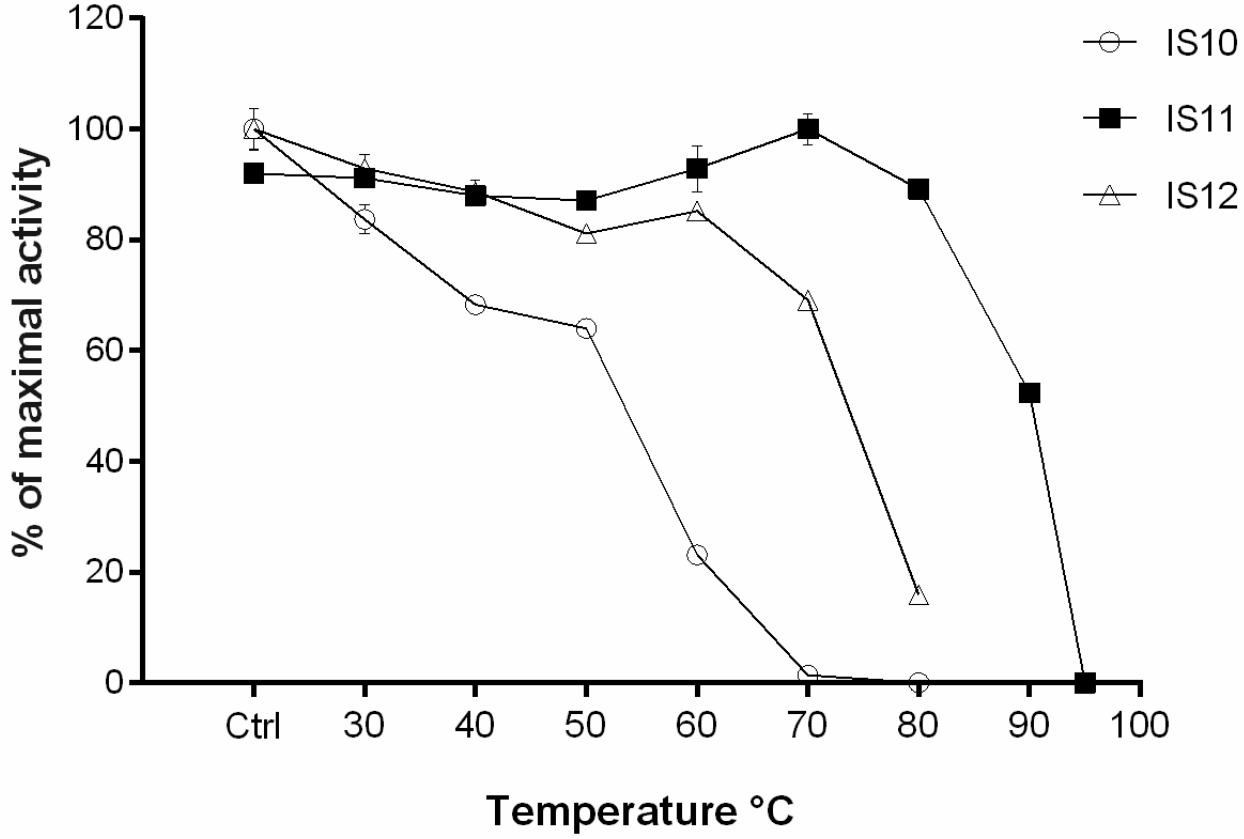
IS10
IS11
IS12
% of maximal activity
0
20
40
60
80
100
120
Ctrl
30
40
50
60
70
80
90
100
Temperature °C

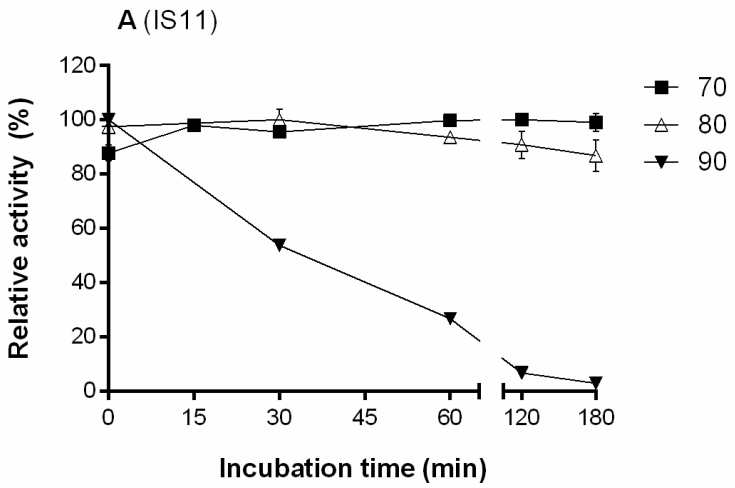
A (IS11)
Relative activity (%)
120
100
80
60
40
20
0
0
15
30
45
60
120
180
Incubation time (min)
70
80
90

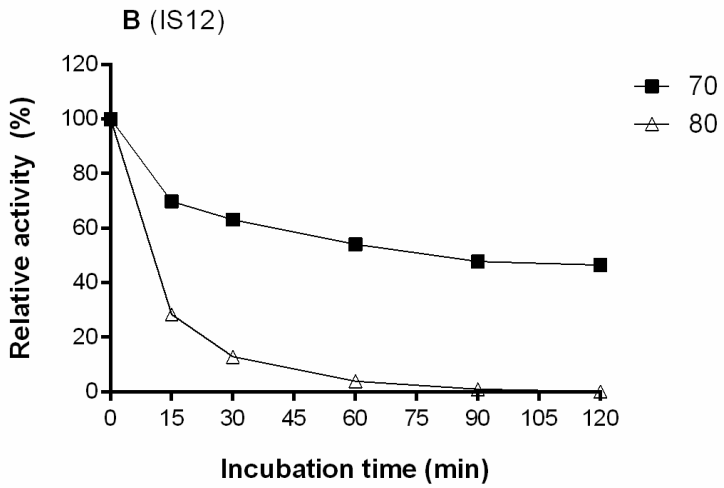
B (IS12)
Relative activity (%)
120
100
80
60
40
20
0
0
15
30
45
60
75
90
105
120
Incubation time (min)
70
80

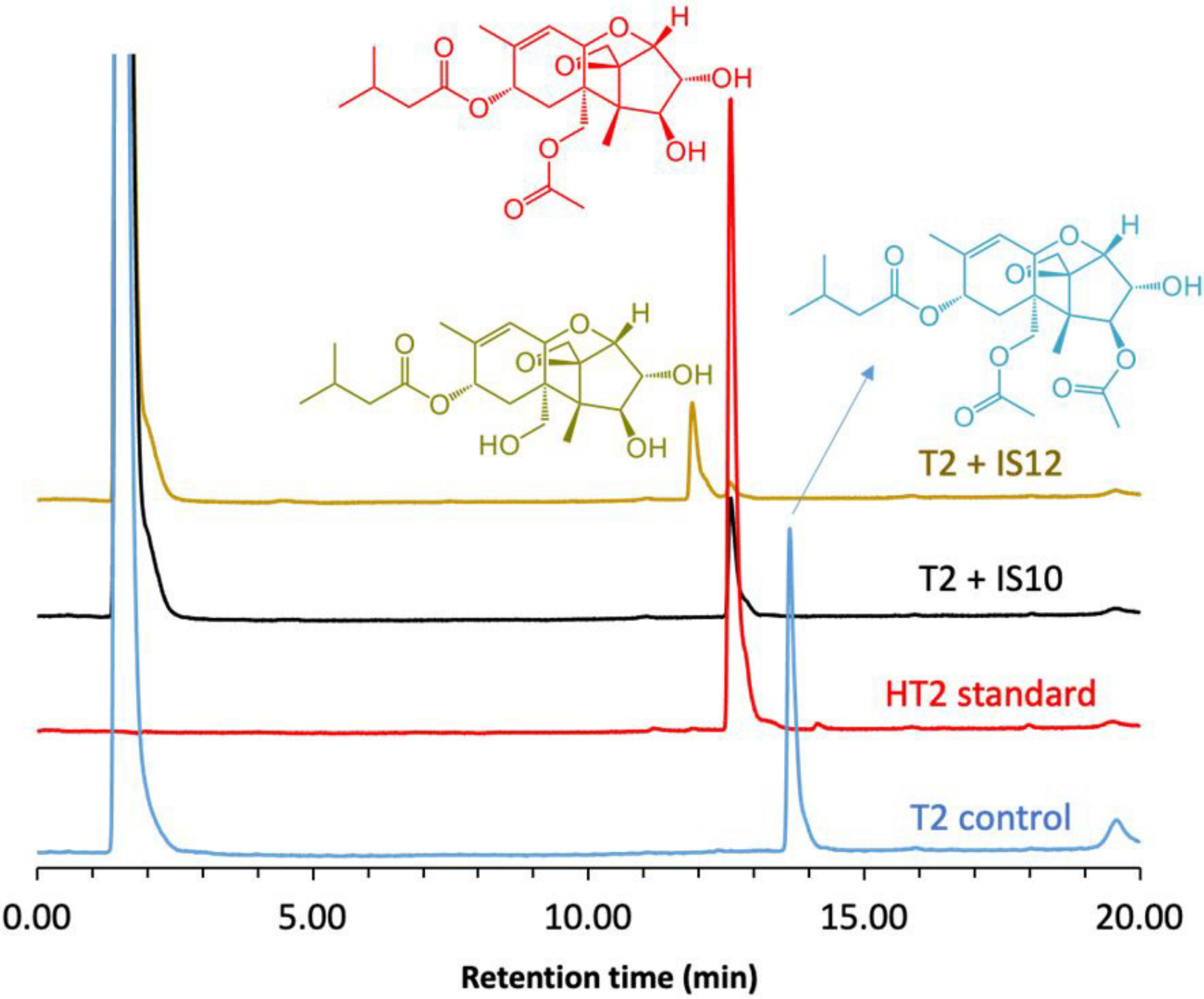
T2 + IS12
T2 + IS10
HT2 standard
T2 control
0.00
5.00
10.00
15.00
20.00
Retention time (min)

A

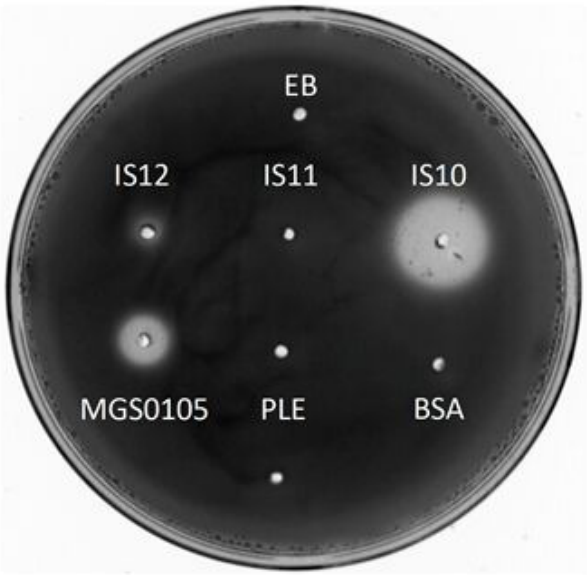
EB
IS12
IS11
IS10
MGS0105
PLE
BSA

B

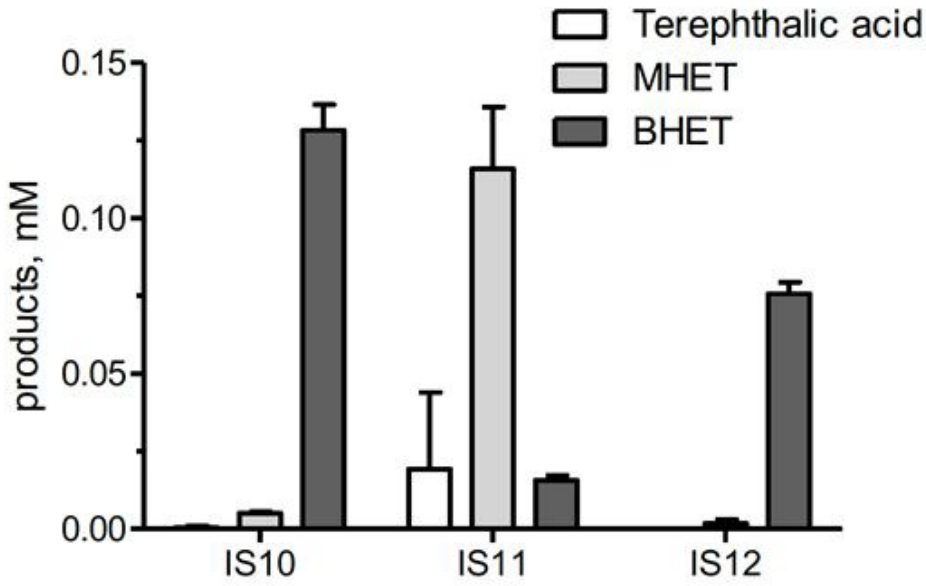
Terephthalic acid
MHET
BHET
products, mM
0.15
0.10
0.05
0.00
IS10
IS11
IS12

C

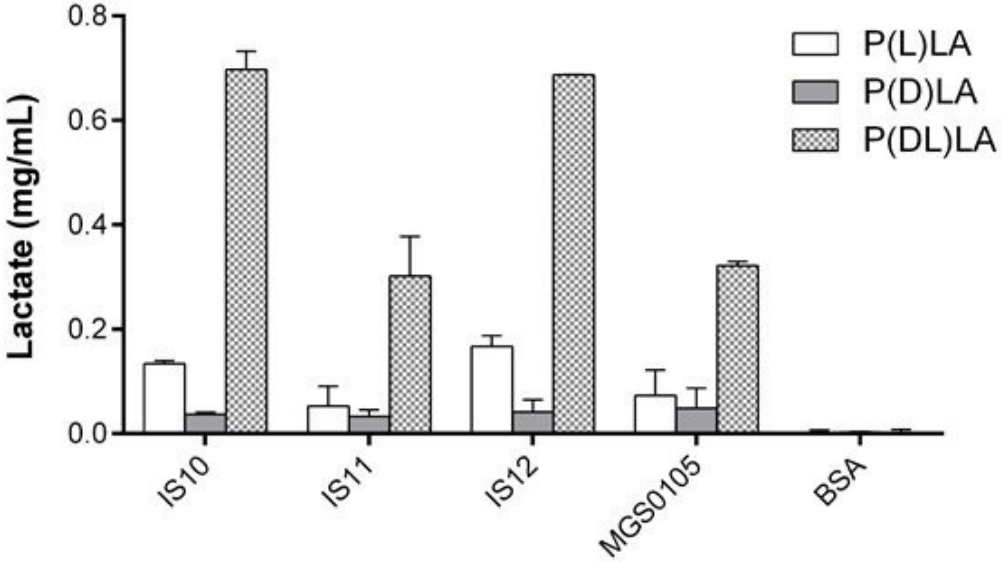
P(L)LA
P(D)LA
P(DL)LA
Lactate (mg/mL)
0.8
0.6
0.4
0.2
0.0
IS10
IS11
IS12
MGS0105
BSA

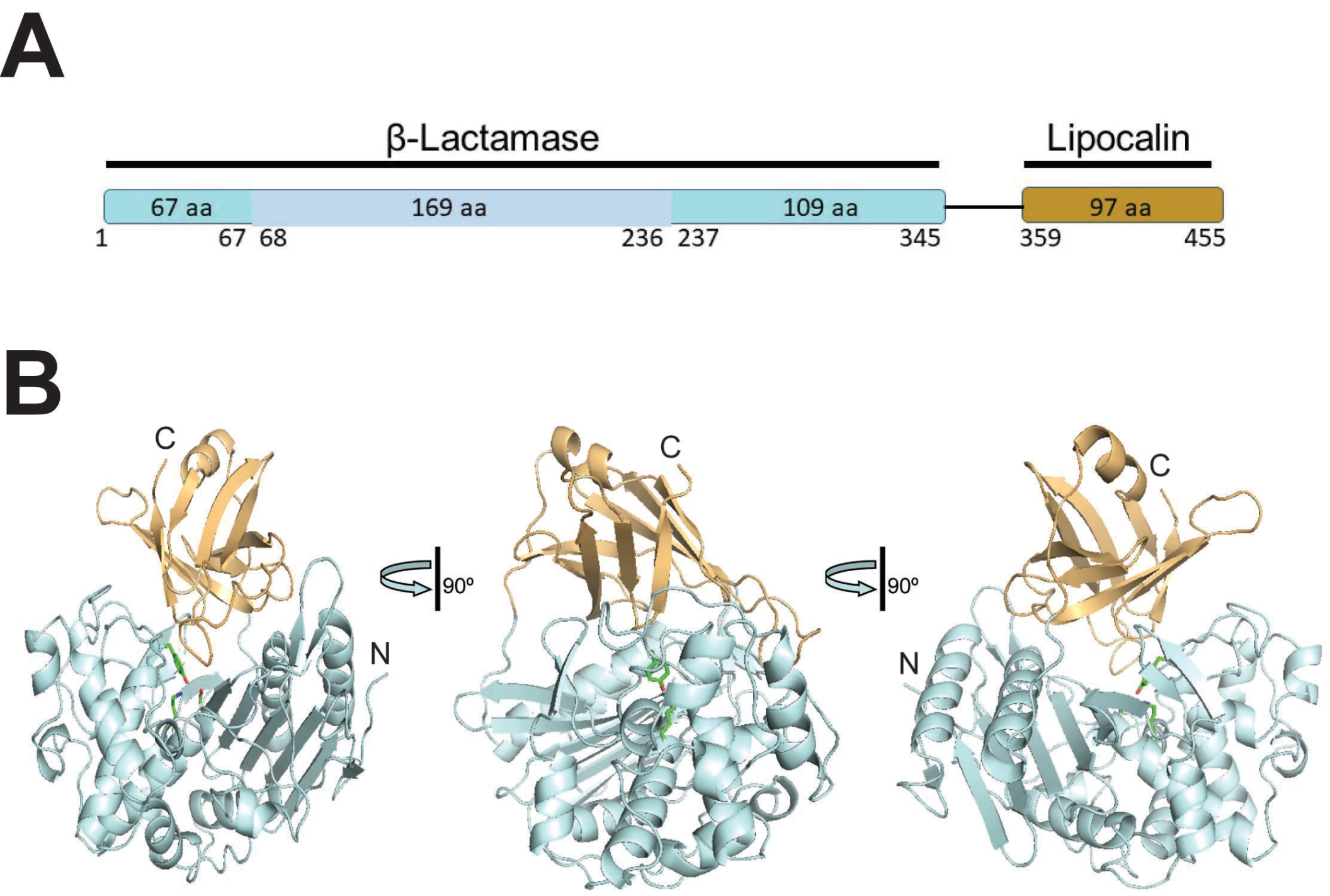
A
β-Lactamase
Lipocalin
67 aa
169 aa
109 aa
97 aa
1
67
68
236
237
345
359
455
B
C
N
90º
C
90º
C
N

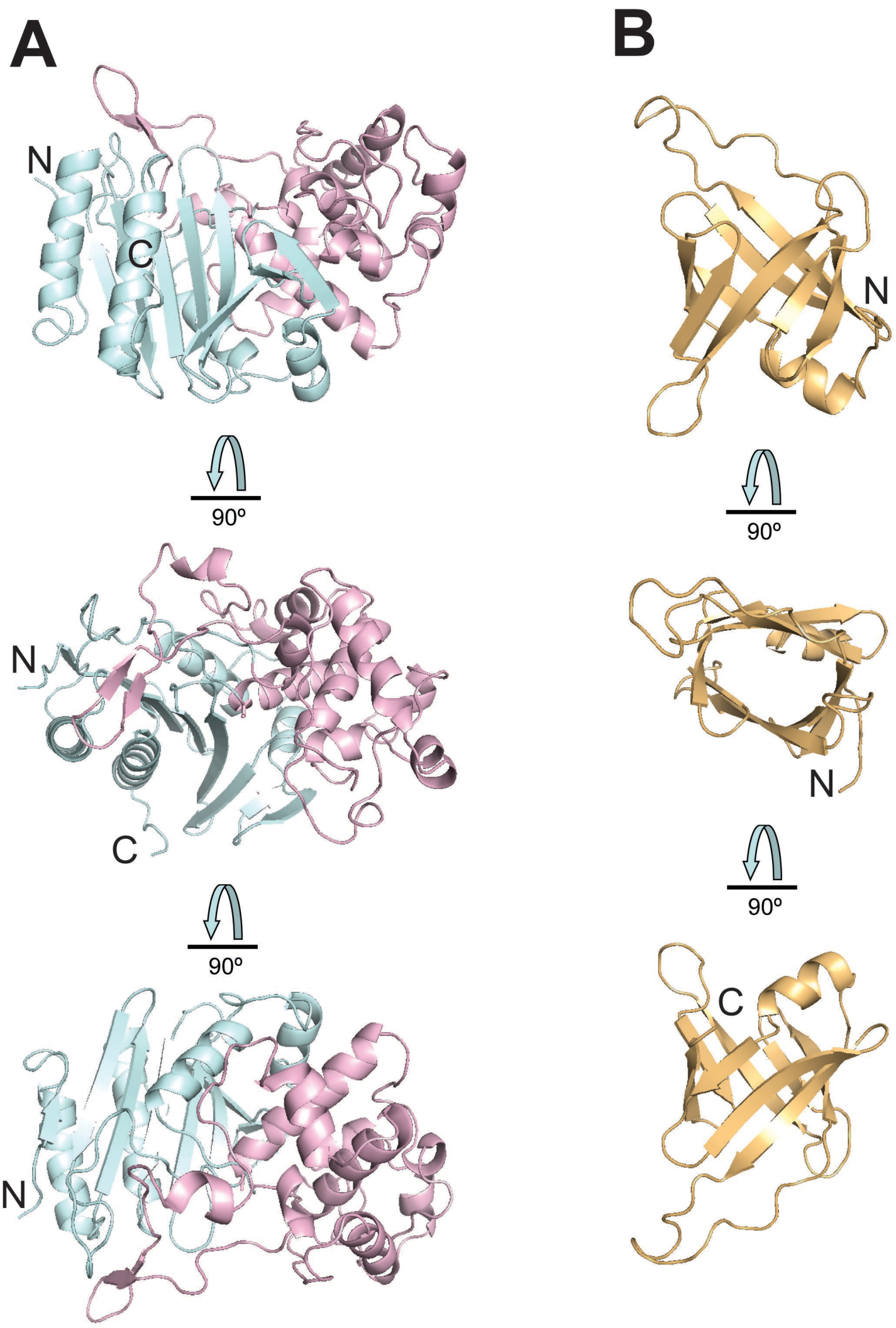
A
B
N
C
90º
N
C
90º
N
N
90º
C
90º

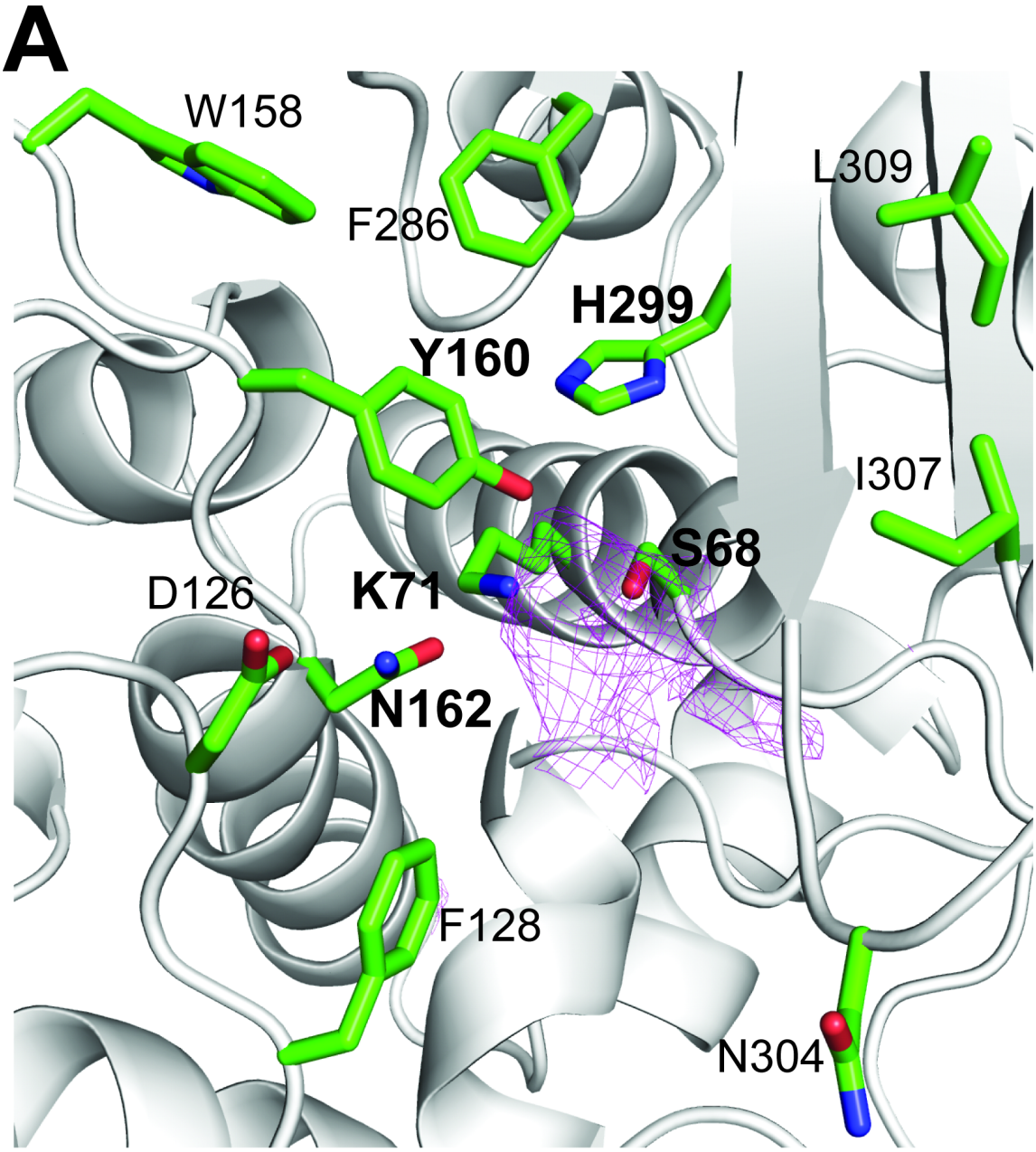
A
W158
F286
L309
H299
Y160
I307
S68
D126
K71
N162
F128
N304

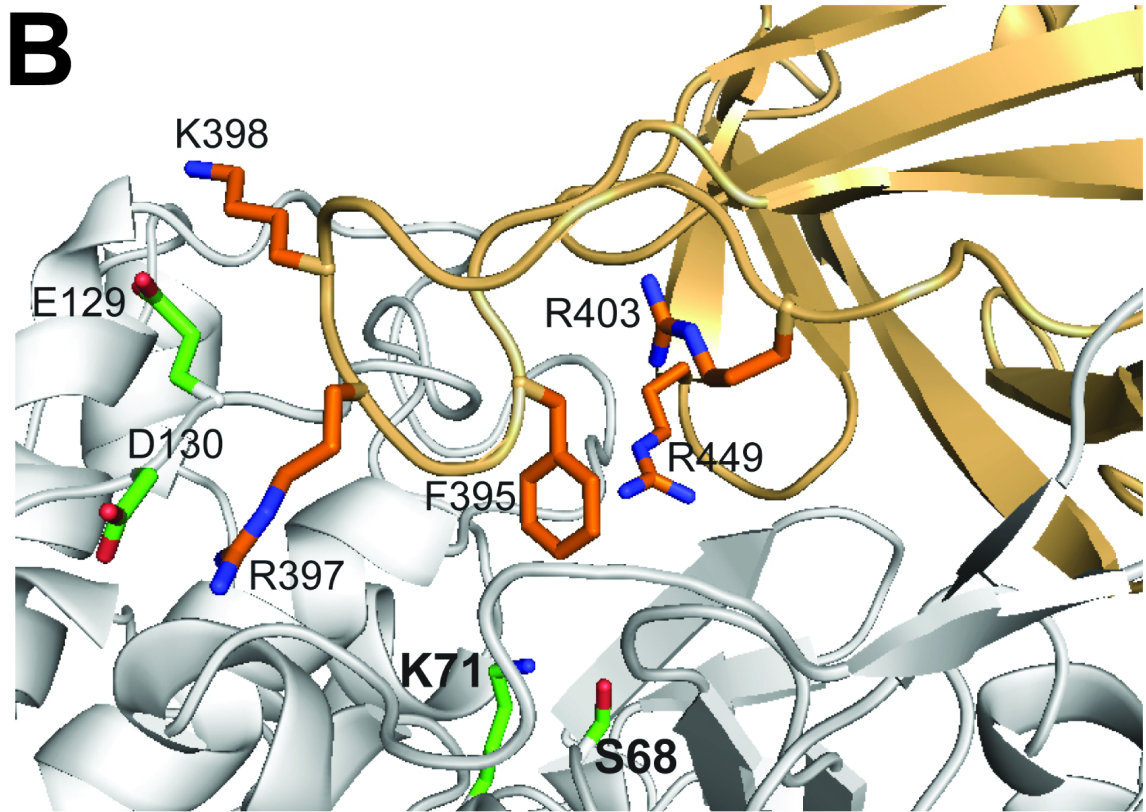
B
K398
E129
R403
D130
R449
F395
R397
K71
S68

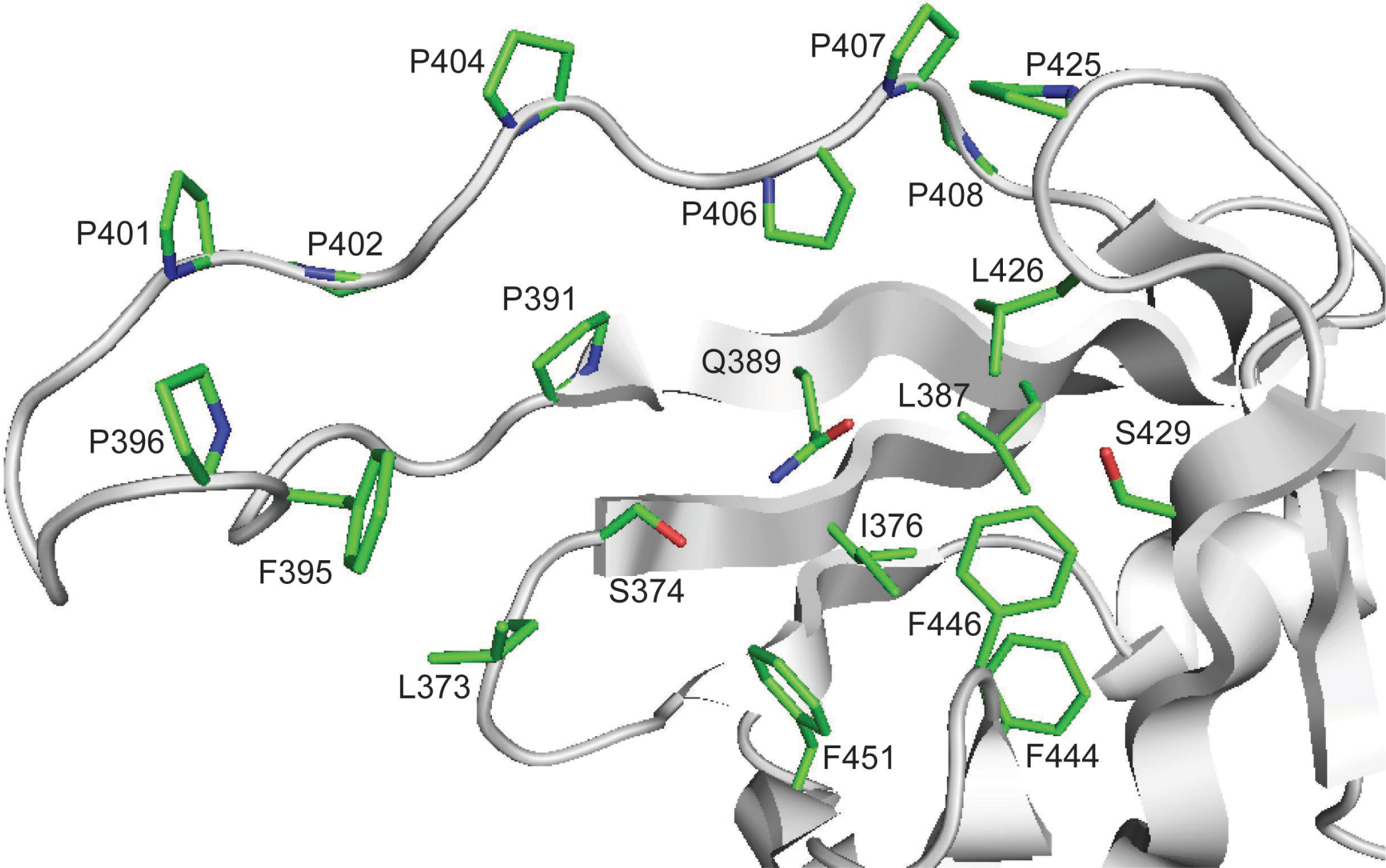
P404
P407
P425
P401
P402
P406
P408
L426
P391
Q389
L387
P396
S429
I376
F395
S374
F446
L373
F451
F444